

1 **Title:** Decadal variation of CO₂ fluxes and its budget in a wheat and maize rotation cropland
2 over the North China Plain

3 Quan Zhang^{1,2}, Huimin Lei², Dawen Yang², Lihua Xiong¹, Pan Liu¹, Beijing Fang^{2,3}

4 ¹State Key Laboratory of Water Resources and Hydropower Engineering Science, Wuhan
5 University, Wuhan, China

6 ²State Key Laboratory of Hydrosience and Engineering, Department of Hydraulic
7 Engineering, Tsinghua University, Beijing, China

8 ³Department of Civil and Environmental Engineering, The Hong Kong University of Science
9 and Technology, Hong Kong SAR, China

10 Correspondence to:

11 Q. Zhang (quan.zhang@whu.edu.cn) and H. Lei (leihm@tsinghua.edu.cn)

12 Tel: 86-(0)10-6278-3383

13 Fax: 86-(0)10-6279-6971

14 **This work is distributed under the Creative Commons Attribution 4.0 License**



16 **Abstract:**

17 Carbon sequestration in agro-ecosystems has great potentials to mitigate global greenhouse
18 gas emissions. To assess the decadal trend of CO₂ fluxes of an irrigated wheat-maize rotation
19 cropland over the North China Plain, the net ecosystem exchange (NEE) with the atmosphere
20 was measured by using an eddy covariance system from 2005 through 2016. To evaluate the
21 detailed CO₂ budget components of this representative cropland, a comprehensive experiment
22 was conducted in the full 2010-2011 wheat-maize rotation cycle by combining the eddy
23 covariance NEE measurements, plant carbon storage samples, a soil respiration experiment
24 that differentiated between heterotrophic and below-ground autotrophic respirations. Over the
25 past decade from 2005 through 2016, the cropland exhibited a non-statistically significant
26 decreasing carbon sequestration capacity; the average of total NEE, Gross Primary
27 Productivity (GPP), Ecosystem Respiration (ER) for wheat were -364, 1174 and 810 gC m⁻²,
28 and were -136, 1008, and 872 gC m⁻² for maize. The multiple regression revealed that, air
29 temperature and groundwater depth showed pronounced correlation with the CO₂ fluxes for
30 wheat; but in the maize season, incoming short-wave radiation and groundwater depth
31 showed pronounced correlations with CO₂ fluxes. For the full 2010-2011 agricultural cycle,
32 the CO₂ fluxes for wheat and maize were as follows: NEE -438 and -239 gC m⁻², GPP 1078
33 and 780 gC m⁻², ER 640 and 541 gC m⁻², soil heterotrophic respiration 377 and 292 gC m⁻²,
34 below-ground autotrophic respiration 136 and 115 gC m⁻², above-ground autotrophic
35 respiration 128 and 133 gC m⁻²; the net biome productivity was 59 gC m⁻² for wheat and 5 gC
36 m⁻² for maize, indicating that wheat was a weak CO₂ sink and maize was close to CO₂ neutral
37 to the atmosphere for this agricultural cycle. However, when considering the total CO₂ loss in

38 the fallow period, the net biome productivity was $-40 \text{ gC m}^{-2} \text{ yr}^{-1}$ for the full 2010-2011
39 cycle, implying that the cropland was a weak CO_2 source. The investigations of this study
40 showed that taking cropland as a climate change mitigation tool is challenging and further
41 studies are required for the CO_2 sequestration potential of croplands.

42 **Key words:** Cropland; CO_2 ; Decadal trend; Maize; North China Plain; Wheat

43 **Introduction**

44 The widely used eddy covariance technique (Aubinet et al., 2000; Baldocchi et al., 2001;
45 Falge et al., 2002b) has enabled us to better understand the terrestrial CO₂ exchange with the
46 atmosphere, thereby forested our understanding of the mechanisms on how the terrestrial
47 ecosystems contribute to mitigate the ongoing climate change (Falkowski et al., 2000; Gray et
48 al., 2014; Poulter et al., 2014; Forkel et al., 2016). Agro-ecosystems play an important role in
49 regulating the global carbon balance (Lal, 2001; Bondeau et al., 2007; Özdoğan, 2011; Taylor
50 et al., 2013; Gray et al., 2014) and are believed to have great potentials to mitigate global
51 carbon emissions through cropland management (Sauerbeck, 2001; Freibauer et al., 2004;
52 Smith, 2004; Hutchinson et al., 2007; van Wesemael et al., 2010; Ciais et al., 2011; Schmidt et
53 al., 2012), furthermore, some studies proposed the agro-ecosystems as the “natural climate
54 solutions” to mitigate global carbon emission (e.g., Griscom et al., 2017; Fargione et al.,
55 2018). The field management practices (e.g., irrigation, fertilization and residue removal, etc.)
56 impact the cropland CO₂ fluxes (Baker and Griffis, 2005; Béziat et al., 2009; Ceschia et al.,
57 2010; Eugster et al., 2010; Drewniak et al., 2015; de la Motte et al., 2016; Hunt et al., 2016;
58 Vick et al., 2016), but their relative importance in determining the cropland CO₂ budget
59 remain unclear because of limited field observations (Kutsch et al., 2010), motivating
60 comprehensive CO₂ budget assessments across different cropland management styles.

61 Over the past two decades, CO₂ investigations of agro-ecosystems have mainly focused on the
62 variations in the net ecosystem exchange with the atmosphere (i.e., NEE) or its two derived
63 components (i.e., GPP and ER) using the eddy covariance. To date, these evaluations have

64 been widely conducted for wheat (Gilmanov et al., 2003; Anthoni et al., 2004a; Moureaux et
65 al., 2008; Béziat et al., 2009; Vick et al., 2016), maize (Verma et al., 2005), sugar beet
66 (Aubinet et al., 2000; Moureaux et al., 2006), potato (Anthoni et al., 2004b; Fleisher et al.,
67 2008), soybean-maize rotation cropland (Gilmanov et al., 2003; Hollinger et al., 2005; Suyker
68 et al., 2005; Verma et al., 2005; Grant et al., 2007), and winter wheat-summer maize cropland
69 (Zhang et al., 2008; Lei and Yang, 2010). However, the long-term variations of the cropland
70 CO₂ fluxes remain limited, leaving our knowledge of the cropland potential as the future
71 climate change mitigation tool incomplete.

72 The widely used eddy covariance technique has fostered our understanding of the integrated
73 fluxes of NEE, GPP and ER, but cannot provide the detailed CO₂ budget components, which
74 consist of carbon assimilation (i.e., GPP), soil heterotrophic respiration (R_H), above-ground
75 autotrophic respiration (R_{AA}), below-ground autotrophic respiration (R_{AB}), lateral carbon
76 export at harvest and import at sowing or through organic fertilization (Ceschia et al., 2010).
77 These different CO₂ components result from different biological and biophysical processes
78 (Moureaux et al., 2008) that may respond differently to climatic conditions, environmental
79 factors and management strategies (Ekblad et al., 2005; Zhang et al., 2013). Differentiating
80 among these components is a prerequisite for understanding the response of terrestrial
81 ecosystems to changing environment (Heimann and Reichstein, 2008), so the carbon budget
82 evaluations have been reported for a few croplands (e.g., Moureaux et al., 2008; Ceschia et
83 al., 2010; Wang et al., 2015; Demyan et al., 2016; Gao et al., 2017). In particular, to account
84 for the literal carbon export, the Net Biome Productivity (NBP) is often estimated by

85 combining the eddy covariance technique and field carbon measurements associated with
86 harvests and residue treatments (Ceschia et al., 2010; Kutsch et al., 2010). As detailed CO₂
87 budget might facilitate better predictions of agro-ecosystems' responses to climate change, the
88 CO₂ budget evaluations in different croplands remain necessary.

89 The North China Plain (NCP) is one of the most important food production regions in China,
90 and it guarantees the national food security by providing more than 50% and 33% of the nation's
91 wheat and maize, respectively (Kendy et al., 2003). Irrigation by diverting water from the
92 Yellow River is common to alleviate the water stress during spring in the NCP, resulting in a
93 very shallow groundwater depth (usually range from 2 to 4 m) along the Yellow River (Cao et
94 al., 2016) (Fig. 1). Wang et al. (2015) suggested that a groundwater-fed cropland in the NCP
95 had been losing carbon, and other studies also reported croplands in this region as carbon
96 sources (e.g., Li et al., 2006; Luo et al., 2008). However, the long-term variations (e.g., >10
97 years) of the CO₂ fluxes over the NCP remain lacking, leaving the trend of carbon sequestration
98 capacity of this region unknown.

99 To this end, this study is designed to assess the long-term variation of CO₂ fluxes and its
100 budget of the representative wheat-maize rotation cropland in the NCP. The eddy covariance
101 system was used to measure the CO₂ exchange from 2005 through 2016. For the full 2010-
102 2011 agricultural cycle, we measured soil respiration and sampled crops to quantify the
103 detailed CO₂ budget components. These measurements allow to (1) investigate the decadal
104 CO₂ flux (NEE, GPP, and ER) trend over this cropland; (2) provide the detailed CO₂ budget
105 components; and (3) estimate the Net Primary Productivity (NPP), Net Ecosystem

106 Productivity (NEP), and NBP.

107 **Materials and methods**

108 **Site description and field management**

109 The experiment was conducted in a rectangular-shaped (460 m × 280 m) field of the
110 representative cropland over the NCP (36° 39' N, 116° 03' E, Weishan site of Tsinghua
111 University, Fig. 1). The soil is silt loam with the field capacity of 0.33 m³ m⁻³ and saturation
112 point of 0.45 m³ m⁻³ for the top 5 cm soil. The mean annual precipitation is 532 mm and the
113 mean air temperature is +13.3 °C. The winter wheat-summer maize rotation system is the
114 representative cropping style in this region. On average, the winter wheat is sown around
115 October 17th and harvested around June 16th of the following year with crop residues left on
116 the field; summer maize is sown following the wheat harvest around June 17th and harvested
117 around October 16th. Prior to sowing wheat of the next season, the field is thoroughly
118 ploughed to fully incorporate maize residues into the top 20 cm soil. The canopies of both
119 wheat and maize are very uniform across the whole season. Nitrogen fertilizer is commonly
120 applied at this site with the amount of 35 gN m⁻² for wheat and 20 gN m⁻² for maize. The crop
121 density is 775 plants m⁻² for wheat with a ridge spacing of 0.26 m, and 4.9 plants m⁻² for
122 maize with a ridge spacing of 0.63 m, on average. Wheat is commonly irrigated with water
123 diverted from the Yellow River and the irrigation is about 150 mm every year; maize is rarely
124 irrigated because of the high precipitation in the summer. During the 2010-2011 agricultural
125 cycle with CO₂ budget components evaluated, winter wheat was sown on October 23rd, 2010
126 and subsequently harvested on June 10th, 2011; summer maize was sown on June 23rd, 2011

127 and harvested on September 30th, 2011. The entire year from October 23rd, 2010 through
128 October 22nd, 2011 was studied for the annual CO₂ budget evaluation.

129 (Fig. 1 here)

130 **Eddy covariance measurements**

131 A flux tower was set up at the center of the experiment field in 2005 (Lei and Yang, 2010;
132 Zhang et al., 2013). The NEE was measured at 3.7m above ground with an eddy covariance
133 system consisting of an infrared gas analyzer (LI-7500, LI-COR Inc., Lincoln, NE, USA) and
134 a three-dimensional sonic anemometer (CSAT3, Campbell Scientific Inc., Logan, UT, USA).
135 The 30-min averaged NEE was calculated from the 10 Hz raw measurements with TK2
136 (Mauder and Foken, 2004) from 2005 through 2012 and TK3 software package (Mauder and
137 Foken, 2011) from 2013 through 2016. The storage flux was calculated by assuming a
138 constant CO₂ concentration profile. Nighttime measurements under stable atmospheric
139 conditions with a friction velocity lower than 0.1 m s⁻¹ were removed from the analysis (Lei
140 and Yang, 2010). In the gap filling procedure, gaps less than 2 h were filled using linear
141 regression, while other short gaps were filled using the Mean Diurnal Variation (MDV)
142 method (Falge et al., 2001); gaps longer than 4 weeks were not filled. NEE was further
143 partitioned to derive GPP and ER using the nighttime method (Reichstein et al., 2005; Lei and
144 Yang, 2010), which assumes that daytime and nighttime ER follow the same temperature
145 response, thereby estimates the daytime ER using the regression model derived from the
146 nighttime measurements. In particular, this study adopted the method proposed by Reichstein
147 (2005) to quantify the short-term temperature sensitivity of ER from nighttime measurements

148 as described by the Vant Hoff equation,

$$149 \quad ER = ER_{\text{ref}} \exp(bT_s), \quad (1)$$

150 Where T_s is soil temperature, ER_{ref} is the reference respiration at 0 °C, and b is a parameter
151 associated with the commonly used temperature sensitivity coefficient Q_{10} ,

$$152 \quad Q_{10} = \exp(10b). \quad (2)$$

153 The long-term temperature sensitivity b of the season (either wheat or maize) was determined
154 by averaging all the estimated short-term b in each of the four-day window with the inverse of
155 the standard error as a weighing factor. The long-term temperature sensitivity b was then used
156 to estimate the ER_{ref} parameter in each of the four-day window by fitting the eq. (1), then
157 ER_{ref} of each day was estimated by using the least square spline approximation (Lei and Yang,
158 2010).

159 To quantify the contribution of source areas to the CO₂ flux measurement of the eddy
160 covariance, we used an analytical footprint model (Hsieh et al., 2000),

$$161 \quad f(\chi, z_m) = \frac{1}{\kappa^2 \chi^2} D z_u^P |L|^{1-P} \exp\left(\frac{-1}{\kappa^2 \chi} D z_u^P |L|^{1-P}\right) \quad (3)$$

162 where $D=0.28$ and $P=0.59$ are similarity constants for unstable condition (Hsieh et al., 2000),
163 $\kappa=0.4$ is von Karman constant, χ represents the horizontal coordinate, L represents the
164 Obukhov length, z_m represents the measurement height, and z_u represents the length scale
165 expressed as,

$$166 \quad z_u = z_m \left[\ln\left(\frac{z_m}{z_0}\right) - 1 + \frac{z_0}{z_m} \right] \quad (4)$$

167 where z_0 represents the roughness height set to be 0.1Hc (canopy height).

168 Note that the eddy covariance system failed from October 23, 2010 to April 1, 2011 during the
169 wheat dormant season. To evaluate the seasonal CO₂ budget of this rotation cycle, the flux
170 gap of this period was filled by using the machine learning Support Vector Regression (SVR)
171 algorithm (Cristianini and Shave-Taylor, 2000), which has been proved to be an appropriate
172 tool for flux gap fillings (e.g., Kang et al., 2019; Kim et al., 2019) (see Appendix A).

173 **Meteorological and environmental condition measurements**

174 The meteorological variables were measured at 30-min intervals by a standard meteorological
175 station on the tower. Among these variables were the air temperature (T_a) and relative
176 humidity (RH) (HMP45C, Vaisala Inc, Helsinki, Finland) at the height of 1.6 m, precipitation
177 (P) (TE525MM, Campbell Scientific Inc), incoming short-wave radiation (R_{si}) (CRN1, Kipp
178 & Zonen, Delft, Netherlands) and photosynthetic photon flux density (PPFD) (LI-190SA, LI-
179 COR Inc) at the height of 3.7 m. The 30-min interval edaphic measurements included soil
180 temperature (T_s) (109-L, Campbell Scientific Inc.), volumetric soil moisture (θ) (CS616-L,
181 Campbell Scientific Inc.) for the top 5 cm soil; soil matric potential (ψ) (257-L, Campbell
182 Scientific Inc.) was measured since 2010 at the same depth. The groundwater depth (WD)
183 (CS420-L, Campbell Scientific Inc.) was measured at a location close to flux tower in 30-min
184 intervals.

185 **Biometric measurements and crop samples**

186 To trace crop development and carbon storage, we measured canopy height (H_c), leaf area
187 index (LAI), crop dry matter (DM), and carbon content of crop organs at an interval of 7-10
188 days in the footprint of eddy covariance. Due to inclement weather, measurement intervals

189 were occasionally extended to two weeks or longer. The Hc was measured with a ruler and
190 LAI was measured with LAI-2000 (LI-COR Inc.) at ten locations randomly distributed in the
191 field. For crop samples, four locations were randomly selected at the start of the growing
192 season, crop samples were then collected close to these four locations throughout the
193 experimental period. At each location, 10 crop samples were collected for wheat and 3 crop
194 samples were collected from maize. To reduce the sample uncertainty at harvest, 200 crops
195 and 5 crops were collected in each location for wheat and maize, respectively. The crop
196 organs were separated and oven-dried at 105 °C for kill-enzyme torrefaction for 30 min, and
197 then oven-dried at 75 °C until a constant weight. The crop samples were used to estimate the
198 average field biomass (Dry Matter). The carbon content was analyzed using the combustion
199 oxidation-titration method (National Standards of Environmental Protection of the People's
200 Republic of China, 2013) to estimate carbon storage. The crop samples provided a direct
201 estimate of the NPP.

202 **Soil respiration measurements**

203 Soil respiration was measured every day in the footprint of the eddy covariance between
204 13:00 and 15:00 from March through September of 2011 using a portable soil respiration
205 system LI-8100 (LI-COR Inc.). Below-ground autotrophic respiration and heterotrophic
206 respiration were differentiated using the root exclusion method (Zhang et al., 2013). The total
207 soil respiration (R_S) and R_H were measured at treatments with and without roots, respectively,
208 and the corresponding difference is R_{AB} . To reduce the uncertainty associated with spatial
209 variability, we set three replicate pairs of comparative treatments (i.e., with root and without

210 root) randomly in the field. The uniform field condition contributes to reduce the
211 measurement uncertainty associated with the spatial variability (see Zhang et al., 2013). To
212 assess the seasonal variations and total amount of soil respirations, the seasonal continuous
213 R_H was constructed using the Q_{10} model by incorporating soil moisture as follows (Zhang et
214 al., 2013):

$$215 \quad R_H = A \exp(BT_s) \cdot f(\theta), \quad (4)$$

$$216 \quad f(\theta) = \begin{cases} 1, & \theta \leq \theta_f \\ a(\theta - \theta_f)^2 + 1, & \theta > \theta_f \end{cases}, \quad (5)$$

217 where θ_f is the field capacity. The parameters were inferred by fitting the R_H and T_s
218 measurements by using the least square method (see Zhang et al., 2013), where $A=1.16$,
219 $B=0.0503$, and $a=-44.9$ (see Zhang et al., 2013). Note that because the plant biomass was
220 negligible before March 14th, during which R_H was set to equal to the ecosystem respiration
221 and the R_{AB} was assumed to be 0. R_{AB} of other periods was estimated based on the R_H
222 measurement and the ratio of the R_{AB} to R_S estimated previously (Zhang et al., 2013), and the
223 continuous R_{AB}/R_S ratio was interpolated from the daily records (Fig. 2). This estimation
224 method is robust because the R_{AB}/R_S ratio is nearly constant around its diurnal average
225 (Zhang et al., 2015b).

226 **(Fig. 2 here)**

227 **Synthesis of the CO₂ budget components**

228 The CO₂ budget components were derived by combining the eddy covariance measurements,
229 soil respiration experiments and crop samples. Eddy covariance-measured NEE is the

230 difference between carbon assimilation (i.e., GPP) and carbon release (i.e., ER). The ER
231 consists of R_H , R_{AB} (i.e., root respiration) and above-ground autotrophic respiration (R_{AA}).
232 The total soil respiration is the sum of R_H and R_{AB} ,

$$233 \quad R_S = R_H + R_{AB}. \quad (6)$$

234 The total autotrophic respiration (R_A) is the difference between the eddy covariance-derived
235 ER and R_H ,

$$236 \quad R_A = ER - R_H. \quad (7)$$

237 The above-ground autotrophic respiration (R_{AA}) is the difference between the eddy
238 covariance-derived ER and R_S in eq. (6),

$$239 \quad R_{AA} = ER - R_S. \quad (8)$$

240 NPP is plant biomass carbon storage, and can be quantified as the difference between GPP
241 and R_A ,

$$242 \quad NPP_{EC} = GPP - R_A, \quad (9)$$

243 where the subscript “EC” represents that the NPP is estimated from the eddy covariance-
244 derived GPP. In parallel, NPP can also be directly inferred from biomass samples as,

$$245 \quad NPP_{CS} = C_{cro}, \quad (10)$$

246 where the subscript “CS” indicates that NPP is based on crop samples, and C_{cro} is the plant
247 biomass carbon storage at harvest. We used the average of the two independent NPPs as the
248 measurement for this site.

249 NEP is commonly estimated by the NEE measurement ($NEP_{EC} = -NEE$). In this study, the crop

250 samples and soil respiration measurements also provided an independent estimate as,

$$251 \quad \text{NEP}_{\text{CS}} = \text{NPP}_{\text{CS}} - R_{\text{H}}. \quad (11)$$

252 We used the average of the two NEPs as the measurement for this site.

253 At this site, there were no fire and insect disturbances, and there was no manure fertilizer
254 application. The carbon input from seeds was negligible, and all crop residues were returned
255 to the field. Thus, NBP can be quantified as the difference between NEP and grain export
256 carbon loss (C_{gra}),

$$257 \quad \text{NBP} = \text{NEP} - C_{\text{gra}}, \quad (12)$$

258 **Results**

259 **Meteorological conditions and crop development**

260 The inter-annual variations of major meteorological variables are shown in Fig. 3, and they
261 showed no clear trend for both wheat and maize seasons. For the full 2010-2011 cycle with
262 comprehensive experiments, the average R_{si} and T_{a} were very close to other years; however,
263 the P during maize season was a little higher than other years (Fig. 3c), leading to a shallow
264 WD in maize season (Fig. 3d). The intra-annual variations of field microclimates for the full
265 2010-2011 cycle are shown in Fig. 4. The seasonal maximum and minimum T_{a} occurred in
266 July and January, respectively, and the variations in vapor pressure deficit (VPD) well
267 followed the T_{a} . The WD mainly followed the irrigation events in winter and spring, but
268 followed P in summer and autumn. In particular, the WD varied from 0 to 3 m throughout the
269 year. The wet soil conditions prohibited the field from experiencing water stress (Fig. 4d)

270 because even the lowest soil matric potential (-187.6 kPa) remained a lot higher than the
271 permanent wilting point of crops (around $-1,500.0$ kPa).

272 **(Fig. 3&4 here)**

273 Fig. 5 shows the seasonal variations in Hc and LAI reflecting the crop development for the
274 full 2010-2011 cycle. The maximum LAI was $4.2 \text{ m}^2 \text{ m}^{-2}$ for wheat and $3.6 \text{ m}^2 \text{ m}^{-2}$ for maize.
275 The variations in Hc and LAI distinguished the different stages of crop development. During
276 the wheat season, the stages of regreening, jointing, booting, heading, and maturity started
277 approximately on March 1st, April 20th, May 1st, May 7th, and June 5th, respectively. The
278 seasonal variations in DM agreed well with the crop stages (Fig. 6), and the wheat biomass
279 mainly accumulated in April and May, while maize biomass mainly accumulated in July and
280 August. The total DM was $1,718 \text{ g m}^{-2}$ for wheat and $1,262 \text{ g m}^{-2}$ for maize at harvest. Upon
281 harvest, the wheat DM was distributed as: 3% root, 43% stem, 9% leaf and 45 % grain, while
282 the maize DM was distributed as: 2% root, 29% stem, 7% green leaf, 5% dead leaf, 4%
283 bracket, 7% cob, and 46% grain. The seasonal average carbon contents of the root, stem,
284 green leaf, dead leaf, and grain were 410, 439, 486, 452 and 457 gC kg^{-1} DM for wheat and,
285 408, 438, 477, 457, and 456 gC kg^{-1} DM for maize (see Table 1 for the seasonal variation).

286 **(Table 1 here)**

287 **(Figs. 5&6 here)**

288 **The inter-annual variations in the NEE, GPP and ER**

289 For the period from 2005 through 2016, if grain export was not considered, the wheat was
290 consistent CO_2 sink as the seasonal total NEEs were consistently negative, and the maize was

291 CO₂ sink in most years except for 2012 and 2013 when NEE was positive (Fig. 7a). NEEs of
292 both wheat and maize fields became less negative during the past decade (though not
293 statistically significant), implying a progressive decline of the carbon sequestration potential
294 of this cropland. The GPPs of both wheat and maize showed an increasing trend, though not
295 statistically significant (Fig. 7b). The ERs of both wheat and maize also showed an increasing
296 trend in these years, but only the trend of maize was significant (Fig. 7c). The decadal average
297 of NEE, GPP and ER were -364 ($SD \pm 98$), $1,174$ ($SD \pm 189$) and 810 ($SD \pm 161$) gC m⁻² for
298 wheat, and -136 ($SD \pm 168$), $1,008$ ($SD \pm 297$), and 872 ($SD \pm 284$) gC m⁻² for maize.

299 The NEE, GPP and ER for both wheat and maize were correlated with the three main
300 environmental variables of R_{si}, T_a and WD using the multiple regression (see Appendix B for
301 details). In the wheat season, T_a showed its relatively greater importance than R_{si} and WD to
302 all the three CO₂ fluxes with a higher T_a increasing both GPP and ER, and also enhancing
303 NEE (more negative) (Fig. 8a); WD correlated negatively with GPP, thereby reduced net
304 carbon uptake (less negative NEE); WD exhibited almost no effect on ER; R_{si} exhibited
305 almost no effect on all the three CO₂ fluxes. Therefore, T_a explained most of the inter-annual
306 variations in NEE, GPP and ER, followed by WD. In the maize season, WD had good
307 correlations with all the three fluxes of GPP, ER, and NEE, where a deeper WD contributed to
308 lower both GPP and ER, and also drive higher net carbon uptake (more negative NEE); T_a
309 showed almost no effect on all the three CO₂ fluxes; R_{si} had a positive correlation with ER,
310 but almost no correlation with GPP (Fig. 8b), ultimately, higher R_{si} in maize season lowered
311 the net carbon uptake (more positive NEE). Overall, R_{si} and WD showed their great

312 importance in influencing the inter-annual variation of maize NEE with R_{si} having a positive
313 correlation and WD having a comparable negative correlation (Fig. 8b).
314 (Figs. 7&8 here)

315 **Intra-annual variations in the NEE, GPP and ER**

316 The Intra-annual variations in NEE, GPP, and ER exhibited a bimodal curve corresponding
317 with the two crop seasons (Fig. 9). All the three CO₂ fluxes were almost in phase, with peaks
318 appearing at the start of May during the wheat season and in the middle of August during the
319 maize season. During some of the winter season, the field still sequestered a small amount of
320 CO₂ because of the weak photosynthesis, which was confirmed by leaf level gas exchange
321 measurement (data not shown). Net carbon emission happened during the fallow periods, in
322 addition to the start of the maize season when the plant was small and high temperature
323 enhanced heterotrophic respiration. During the wheat season, two evident spikes appeared on
324 April 21st and May 8th with positive NEE values (i.e., net carbon release). These spikes
325 resulted from the radiation decline during the inclement weather (Fig. 4b), which suppressed
326 the photosynthesis rate; similar phenomena also appeared during the maize season.

327 **(Fig. 9 here)**

328 Fig. 10 shows the variations in ER and its components. During the wheat season, the variation
329 in ER closely followed crop development and temperature, but there were two evident
330 declines at the end of April and the start of May due to low temperatures associated with the
331 inclement weather. During the early growing stage of maize, R_H was the main component of
332 ER. When water logging conditions occurred in late August and early September, both R_H and

333 R_{AB} were suppressed to zero.

334 **(Fig. 10 here)**

335 **CO₂ budget synthesis in the 2010-2011 agricultural cycle**

336 CO₂ budget analysis showed that this wheat-maize rotation cropland has the potential to
337 uptake carbon from the atmosphere (Fig. 11). In the full 2010-2011 cycle, the total NEE, GPP
338 and ER values were -438 , 1078 , and 640 gC m⁻² for wheat, and -239 , 780 and 541 gC m⁻² for
339 maize. The NPP values were 750 and 815 gC m⁻² for wheat based on crop sample and the
340 eddy covariance complemented with soil respiration measurements, respectively, and were
341 592 and 532 gC m⁻² for maize based on the two methods. We used the average of these two
342 methods for NPP measurements, which were 783 (SD ± 46) gC m⁻² for wheat and 562 (SD \pm
343 43) gC m⁻² for maize. We also used the average of NEP by two independent methods for the
344 measurement, and the NEP was 406 gC m⁻² for wheat and 269 gC m⁻² for maize. Furthermore,
345 when considering the carbon loss associated with the grain export, the NBP values were 59
346 gC m⁻² for wheat and 5 gC m⁻² for maize, respectively. Considering the net CO₂ loss of -104
347 gC m⁻² during the two fallow periods, NBP of the whole wheat-maize crop cycle was -40 gC
348 m⁻² yr⁻¹, suggesting that the cropland was a weak carbon source to the atmosphere under the
349 specific climatic conditions and field management practices.

350 **(Fig. 11 here)**

351 **Discussion**

352 This study investigated the decadal variations of the NEE, GPP and ER over an irrigated wheat-
353 maize rotation cropland over the North China Plain, and the results exhibited a decreasing trend

354 of the CO₂ sink capacity during the past decade. The inter-annual variations of the carbon fluxes
355 of wheat showed close dependence on temperature and groundwater depth, while those of maize
356 were mostly regulated by the solar radiation and groundwater depth. Furthermore, the detailed
357 CO₂ budget components were quantified for a full wheat-maize agricultural cycle. Investigating
358 the decadal trend of the CO₂ fluxes and quantifying the detailed CO₂ budget components for
359 this representative cropland will provide useful knowledge for the regional greenhouse gas
360 emission evaluation over the North China Plain.

361 **Comparison with other croplands**

362 The cropland has been reported as carbon neutral to the atmosphere (e.g., Ciais et al., 2010),
363 carbon source (e.g., Anthoni et al., 2004a; Verma et al., 2005; Kutsch et al., 2010; Wang et al.,
364 2015; Eichelmann et al., 2016), and also carbon sink (e.g., Kutsch et al., 2010). Such
365 inconsistency probably results from the different crop types and management practices
366 (residue removal, the use of organic manure, etc.), in addition to variations in the climatic
367 conditions (Béziat et al., 2009; Smith et al., 2014) and fallow period length (Dold et al.,
368 2017). Our results show that the fully irrigated wheat-maize rotation cropland with a shallow
369 groundwater depth was a weak CO₂ sink during both the wheat and maize seasons in the full
370 2010-2011 cycle, but the CO₂ loss during the fallow period reversed the cropland from a sink
371 into a weak source with an NBP of $-40 \text{ gC m}^{-2} \text{ yr}^{-1}$. These results are consistent with previous
372 studies that reported the wheat-maize rotation cropland as a carbon source (Li et al., 2006;
373 Wang et al., 2015). However, the net CO₂ loss was much lower at our site, most likely due to
374 the shallow groundwater depth.

375 Field measurements of the long term of CO₂ fluxes over croplands remain lacking, and we
376 found the carbon sequestration capacity of this cropland has been progressively decreasing,
377 though it was not statistically significant. The cropland has been widely suggested as a
378 climate change mitigation tool (e.g., Lal, 2001), but the potential in the future is challenging.
379 However, since the cropland management greatly impacts the carbon balance of cropland
380 (Béziat et al., 2009; Ceschia et al., 2010), it remains required investigating if the management
381 adjustment can foster the cropland carbon sink capacity over the long term.

382 The annual total NPP of 1,345 gC m⁻² yr⁻¹ at our site is approximately twice the average of
383 the model-estimated NPP for Chinese croplands (714 gC m⁻² yr⁻¹) with a rotation index of 2
384 (i.e., two crop cycles within one year) (Huang et al., 2007), more than three times the value
385 estimated by MODIS (400 gC m⁻² yr⁻¹) (Zhao et al., 2005), and slightly higher than the value
386 of the same crop rotation at the Luancheng site (1,144 gC m⁻² yr⁻¹) (Wang et al., 2015). The
387 higher NPP at our site may partially result from the sufficient irrigation and fertilization
388 (Huang et al., 2007; Smith et al., 2014).

389 The contrasting respiration partitioning of the same crop in different regions (Table 2) indicate
390 that the respiration processes may also be subject to climatic conditions and management
391 practices. Though the ecosystem respiration to GPP at our site is comparable to other studies,
392 the ratio of autotrophic respiration to GPP is much lower at our site, while the ratio of
393 heterotrophic respiration to ecosystem respiration is greater at our site, these findings are
394 different from those at the other sites with similar crop variety (Moureaux et al., 2008;
395 Aubinet et al., 2009; Suleau et al., 2011; Wang et al., 2015; Demyan et al., 2016), as they
396 showed that ecosystem respiration is usually dominated by below-ground and above-ground

397 autotrophic respirations. The higher soil heterotrophic respiration at our site probably results
398 from the full irrigation and shallow groundwater which alleviates soil water stress.

399 **(Table 2 here)**

400 **The effects of groundwater on carbon fluxes**

401 The groundwater table at our site is much closer to the surface because of the irrigation by
402 water diverted from the Yellow River, in contrast, the nearby Luancheng site (Wang et al.,
403 2015) is groundwater-fed with a very deep groundwater depth (approximately 42 m) (Shen et
404 al. 2013), and their CO₂ budget components had some difference with our study. Comparing
405 the net CO₂ exchange of wheat, the GPP at our site is a little higher than the Luancheng site,
406 implying the irrigation at our site may better sustain the photosynthesis rate for wheat; ER at
407 our site is also a little higher than Luancheng site. For maize, both sites are not irrigated due
408 to the high summer precipitation, GPP and ER at our site were comparable to Luancheng site,
409 implying that the irrigation method prior to the maize season had no discernible effect on the
410 integrated CO₂ fluxes for maize. However, the three components of ER in our study showed
411 pronounced difference from the Luancheng site, where they reported the R_{AA} was 411 gC m⁻²
412 for wheat and 428 gC m⁻² for maize, three times the results of our study (128 gC m⁻² for wheat
413 and 133 gC m⁻² for maize). However, their R_{AB} for wheat (36 gC m⁻²) and maize (16 gC m⁻²)
414 were less than a quarter of our results (136 gC m⁻² for wheat and 115 gC m⁻² for maize). Their
415 R_H of wheat (245 gC m⁻²) was less than our estimate (377 gC m⁻²), but R_H of maize (397 gC
416 m⁻²) was greater than our result (292 gC m⁻²). In general, the crop above-ground parts in our
417 site respired more carbon than the Luancheng site, possibly because the shallow groundwater

418 depth at our site increased the above-ground biomass allocation but lowered the root biomass
419 allocation (Poorter et al., 2012). These independent cross-site comparisons demonstrate that
420 carbon budget components may be subject to the specific groundwater depth influenced by
421 the irrigation type, and even the same crop under similar climatic conditions can behave
422 differently in carbon consumption.

423 Our site experienced a short period of water logging during the 2010-2011 cycle due to the
424 combined effects of full irrigation and the high precipitation during the summer. This distinct
425 field condition reduced soil carbon losses in the maize season, potentially maintaining the
426 CO₂ captured by the cropland. Water logging events were occasionally reported in upland
427 croplands, for example, Terazawa et al. (1992) and Iwasaki et al. (2010) suggested that water
428 logging causes damage to plants, resulting in a decline in GPP as reported by Dold et al.
429 (2017) and our study. Our study further shows that water logging reduces ER to a greater
430 degree than GPP possibly because of the low soil oxygen conditions, thereby reduces the
431 overall cropland CO₂ loss. However, the CH₄ release in the short period may be pronounced
432 in water-logged soils. As CH₄ emission in this kind of cropping system over the North China
433 Plain cropland remains lacking, additional field experiments are required to understand how
434 irrigation and water saturation field condition impact the overall carbon budget.

435 **Uncertainty in the estimation and limitation of this study**

436 In the comprehensive experiment period for the full 2010-2011 agricultural cycle, the NEE of
437 wheat season from October 23rd, 2010 to April 1st, 2011 was calculated using a calibrated
438 SVR model. The SVR model performs well in predicting GPP and ER with very high R² of

439 0.95 and 0.97 and an acceptable uncertainty level of 22.9% and 15.2% for GPP and ER,
440 respectively. Hence, these estimates should have a negligible effect on the seasonal total
441 carbon evaluation. The footprint analysis showed that 90% of the measured eddy flux comes
442 from the nearest 420 m and 166 m in wheat and maize crops under unstable conditions,
443 respectively, confirming that both soil respiration experiments and crop samples well paired
444 with the EC measurements.

445 Root biomass was difficult to measure, but the uncertainty should be low, because the root
446 ratio (the ratio of the root weight to the total biomass weight) accounts for 15-16 % of the
447 crop for wheat and maize (Wolf et al., 2015), and our measurements are very close to these
448 values, i.e., the averaged seasonal root ratio was 15% for wheat and 10% for maize at our site.
449 However, the relatively low root ratios (3% for wheat and 2% for maize) at harvest probably
450 result from the root decay associated with plant senescence. The estimates of annual soil
451 respiration are based on the Q_{10} model validated by the field measurements that may generate
452 some uncertainty in the soil respiration budget due to the hysteresis response of soil
453 respiration to temperature (Phillips et al., 2011; Zhang et al., 2015a; Zhang et al., 2018).
454 However, the Q_{10} model remains robust in soil respiration estimations if well validated (Tian
455 et al., 1999; Zhang et al., 2013; Latimer and Risk, 2016), allowing the confidence in the
456 estimates.

457 During the wheat season, the cumulative curves of NPP_{EC} and NPP_{CS} were not perfectly
458 consistent in the main growing season as clear differences emerged during the dormant season
459 of wheat from December 15th, 2010 to March 8th, 2011 (Fig. 12). These differences may result

460 from the small wheat sample number. However, the sample number at harvest was sufficiently
461 big and no discernible difference was found between the two NPPs at harvest. These two
462 independent estimates of NPP were similar throughout the maize season (Fig. 12).

463 This study provides a comprehensive quantification of the CO₂ budget components of the
464 cropland, but it remains limited to a relatively wet year (see Fig. 3c and d). The integrated
465 carbon fluxes (NEE, GPP and ER) have pronounced inter-annual variations, also suggesting
466 further investigations are required on the inter-annual variations of the carbon budget
467 components.

468 **(Fig. 12 here)**

469 **Conclusion**

470 Based on the decadal measurements of CO₂ fluxes over an irrigated wheat-maize rotation
471 cropland over the North China Plain, we found the cropland was a strong CO₂ sink if grain
472 export was not considered. When considering the grain export, the cropland was a weak CO₂
473 source with the NBP of $-40 \text{ gC m}^{-2} \text{ yr}^{-1}$ in the full 2010-2011 agricultural cycle. The net CO₂
474 exchange during the past decade from 2005 through 2016 showed a non-statistically
475 significant decreasing trend, implying a decreasing carbon sequestration capacity of this
476 cropland, discouraging the potential of taking agro-ecosystems as the mitigation tool of
477 climate change. In the wheat season, air temperature showed the best correlation with the CO₂
478 fluxes followed by the groundwater depth; while in the maize season, both short-wave
479 radiation and groundwater depth showed good correlation with the CO₂ fluxes. The
480 comprehensive investigation showed most of the carbon sequestration occurred during the

481 wheat season, while maize was close to being CO₂ neutral. Soil heterotrophic respiration in
482 this cropland contributes substantially to CO₂ loss in both wheat and maize season. This study
483 provides detailed knowledge for estimating regional carbon emission over the North China
484 Plain.

485 **Appendix A. Flux calculation of the period with equipment failure**

486 A1. Support Vector Regression method

487 Support Vector Regression (SVR) method is a machine-learning technique-based regression,
488 which transforms regression from nonlinear into linear by mapping the original low-
489 dimensional input space to higher-dimensional space (Cristianini and Shave-Taylor, 2000).
490 SVR method has two advantages: 1) the model training always converges to global optimal
491 solution with only a few free parameters to adjust, and no experimentation is needed to
492 determine the architecture of SVR; 2) SVR method is robust to small errors in the training data
493 (Ueyama et al., 2013). The SVM software package obtained from LIBSVM (Chang and Lin,
494 2005) is used in this study.

495 A2. Data processing and selection of explanatory variables

496 Gross Primary Productivity (GPP) is influenced by several edaphic, atmospheric, and
497 physiological variables, among which air temperature (T_a), relative humidity (RH), llant area
498 index (LAI), net photosynthetically active radiation (PAR), and soil moisture (θ) are the
499 dominant factors. Hence, we select T_a , RH, LAI, PAR, and θ as explanatory variables of GPP.
500 Ecosystem Respiration (ER) consists of total soil respiration and above-ground autotrophic
501 respiration. The total soil respiration is largely influenced by soil temperature and soil moisture,
502 while above-ground autotrophic respiration is largely influenced by air temperature and above-
503 ground biomass. So we select T_a , soil temperature at 5 cm (T_s), θ and LAI as explanatory
504 variables of ER. LAI is estimated from the Wide Dynamic Range Vegetation Index derived
505 from the MOD09Q1 reflectance data (250 m, 8-d average,

506 https://lpdaac.usgs.gov/dataset_discovery/modis/modis_products_table/mod09q1, also see Lei
507 et al. 2013).

508 The three wheat seasons of 2005-2006, 2009-2010, and 2010-2011 are selected for model
509 training, and the original half-hourly measurements of GPP and ER together with the
510 explanatory variables are averaged to the daily scale, but we remove days missing more than
511 25% of half-hourly data. We have GPP available from 466 days and ER from 483 days for
512 model training. The explanatory variables for the equipment failure are also averaged into daily
513 scale, which will be used to calculate GPP and ER with the trained model described in the
514 following section.

515 A3. SVR model training and flux calculation

516 In order to eliminate the impact of variables with different absolute magnitudes, we rescale all
517 the variables in training-data set to the [0, 1] range prior to SVR model training. In the training
518 process, the radial basis function (RBF, a kernel function of SVR) is used and the width of
519 insensitive error band is set as 0.01. The SVR model training follows these steps:

520 (1) All training data samples are randomly divided into five non-overlapping subsets, and four
521 of them are selected as the training sets (also calibration set), the remaining subset is treated as
522 the test set (also validation set). Such process is repeated five times to ensure that every subset
523 has a chance to be the test set.

524 (2) For the selected training set, the SVR parameters (cost of errors c and kernel parameter σ)
525 are determined using a grid search with a five-fold cross-validation training process. In this
526 approach, the training set is further randomly divided into five non-overlapping subsets.

527 Training is performed on each of the four subsets within this training set, with the remaining
528 subset reserved for calculating the Root Mean Square Error (RMSE), and model parameters (c
529 and σ) yielding the minimum RMSE value are selected.

530 (3) The SVR model is trained based on the training set from step (1) and initialized by the
531 parameters (c and σ) derived from step (2).

532 (4) The test set from the step (1) is used to evaluate the model obtained from the step (3) by
533 using the coefficient of determination (R^2) and RMSE.

534 (5) The model is trained with all of the available samples with good performance achieved, as
535 R^2 are 0.95 and 0.97 for GPP and ER, respectively, and the mean RMSE are $1.28 \text{ gC m}^{-2} \text{ d}^{-1}$
536 and $0.44 \text{ gC m}^{-2} \text{ d}^{-1}$. The RMSE can be further used as a metric quantifying uncertainty, which
537 accounts for 22.9% and 15.2% for the averaged GPP and ER, respectively. GPP and ER during
538 equipment failure period are then calculated with the trained model complemented with the
539 observed explanatory variables, and NEE is derived as the difference of GPP and ER.

540 **Appendix B. Multiple regression for NEE, GPP and ER with microclimate variables**

541 The flux of NEE, GPP or ER is correlated with incoming short-wave radiation (R_{si}), air
542 temperature (T_a) and groundwater depth (WD) as $\text{flux} = aR_{si} + bT_a + cWD + d$, where flux is NEE,
543 GPP, or ER; a , b , c , and d are regression parameters. All the variables are normalized to derive
544 their z-score before the regression, where z-score is to subtract the mean from the data and
545 divide the result by standard deviation. The coefficient of each variable represents the relative
546 importance of the corresponding variable in contributing to the dependent variable.

547

548 **Data availability**

549 The data of this study are available for public after a request to the corresponding author (H.
550 Lei).

551 **Author contributions**

552 Q.Z. and H.L. designed the study and methodology with substantial input from all co-authors.
553 Q.Z. conducted the field experiment. B.F. conducted the SVR calculation for gap filling. All
554 authors contributed to interpretation of the results. Q.Z. drafted the manuscript, and all authors
555 edited and approved the final manuscript.

556 **Competing interests**

557 The authors declare that they have no conflict of interest.

558 **Acknowledgement**

559 We thank editor P. C. Stoy, reviewers Dr. R. Scott and S. Spawn for their constructive
560 comments, which greatly improved this work. We also would like to thank two additional
561 anonymous reviewers of the initial submission, and we could not have achieved this without
562 their constructive criticism. This research was supported by the NSFC-NSF collaboration (P.
563 R. China-U.S.) funding (No. 51861125102), National Natural Science Foundation of China
564 (Project Nos. 51509187, 51679120 and 51525902), which are greatly appreciated.

565 **Reference**

566 Anthoni, P. M., Freibauer, A., Kolle, O., and Schulze, E. D.: Winter wheat carbon exchange in
567 Thuringia, Germany, *Agric. For. Meteorol.*, 121, 55-67, doi: 10.1016/s0168-1923(03)00162-
568 x, 2004a.

569 Anthoni, P. M., Knohl, A., Reibmann, C., Freibauer, A., Mund, M., Ziegler, W., Kolle, O., and

570 Schulze, E. D.: Forest and agricultural land-use-dependent CO₂ exchange in Thuringia,
571 Germany, *Global Change Biol.*, 10, 2005-2019, doi: 10.1111/j.1365-2486.2004.00863.x,
572 2004b.

573 Aubinet, M., Grelle, A., Ibrom, A., Rannik, Ü., Moncrieff, J., Foken, T., Kowalski, A. S.,
574 Martin, P. H., Berbigier, P., Bernhofer, C., Clement, R., Elbers, J., Granier, A., Grunwald,
575 T., Morgenstern, K., Pilegaard, K., Rebmann, C., Snijders, W., Valentini, R., and Vesala, T.:
576 Estimates of the annual net carbon and water exchange of forests: The EUROFLUX
577 methodology, *Adv. Ecol. Res.*, 30, 113-175, 2000.

578 Aubinet, M., Moureaux, C., Bodson, B., Dufranne, D., Heinesch, B., Suleau, M., Vancutsem,
579 F., and Vilret, A.: Carbon sequestration by a crop over a 4-year sugar beet/winter wheat/seed
580 potato/winter wheat rotation cycle, *Agric. For. Meteorol.*, 149, 407-418, doi:
581 10.1016/j.agrformet.2008.09.003, 2009.

582 Baker, J. M., and Griffis, T. J.: Examining strategies to improve the carbon balance of
583 corn/soybean agriculture using eddy covariance and mass balance techniques, *Agric. For.*
584 *Meteorol.*, 128, 163-177, doi: 10.1016/j.agrformet.2004.11.005, 2005.

585 Baldocchi, D., Falge, E., Gu, L. H., Olson, R., Hollinger, D., Running, S., Anthoni, P.,
586 Bernhofer, C., Davis, K., Evans, R., Fuentes, J., Goldstein, A., Katul, G., Law, B., Lee, X.
587 H., Malhi, Y., Meyers, T., Munger, W., Oechel, W., U, K. T. P., Pilegaard, K., Schmid, H.
588 P., Valentini, R., Verma, S., Vesala, T., Wilson, K., and Wofsy, S.: FLUXNET: A new tool
589 to study the temporal and spatial variability of ecosystem-scale carbon dioxide, water vapor,
590 and energy flux densities, *B Am. Meteorol. Soc.*, 82, 2415-2434, 2001.

591 Béziat, P., Ceschia, E., and Dedieu, G.: Carbon balance of a three crop succession over two
592 cropland sites in South West France, *Agric. For. Meteorol.*, 149, 1628-1645, doi:
593 10.1016/j.agrformet.2009.05.004, 2009.

594 Bondeau, A., Smith, P. C., Zaehle, S., Schaphoff, S., Lucht, W., Cramer, W., Gerten, D., Lotze-
595 Campen, H., Muller, C., Reichstein, M., and Smith, B.: Modelling the role of agriculture for
596 the 20th century global terrestrial carbon balance, *Global Change Biol.*, 13, 679-706, doi:
597 10.1111/j.1365-2486.2006.01305.x, 2007.

598 Cao, G., Scanlon, B.R., Han, D. and Zheng, C.: Impacts of thickening unsaturated zone on
599 groundwater recharge in the North China Plain. *J. Hydrol.*, 537, 260-270, doi:
600 10.1016/j.jhydrol.2016.03.049, 2016.

601 Ceschia, E., Béziat, P., Dejoux, J. F., Aubinet, M., Bernhofer, C., Bodson, B., Buchmann, N.,
602 Carrara, A., Cellier, P., Di Tommasi, P., Elbers, J. A., Eugster, W., Grunwald, T., Jacobs, C.
603 M. J., Jans, W. W. P., Jones, M., Kutsch, W., Lanigan, G., Magliulo, E., Marloie, O., Moors,
604 E. J., Moureaux, C., Olioso, A., Osborne, B., Sanz, M. J., Saunders, M., Smith, P., Soegaard,
605 H., and Wattenbach, M.: Management effects on net ecosystem carbon and GHG budgets at
606 European crop sites, *Agric. Ecosyst. Environ.*, 139, 363-383, doi:
607 10.1016/j.agee.2010.09.020, 2010.

608 Chang, C. C., and Lin, C. J.: LIBSVM-A library for Support Vector Machines.
609 <http://www.csie.ntu.edu.tw/~cjlin/libsvm/>, 2005.

610 Chen, Y. L., Luo, G. P., Maisupova, B., Chen, X., Mukanov, B. M., Wu, M., Mambetov, B. T.,
611 Huang, J. F., and Li, C. F.: Carbon budget from forest land use and management in Central

612 Asia during 1961-2010, *Agric. For. Meteorol.*, 221, 131-141, doi:
613 10.1016/j.agrformet.2016.02.011, 2016.

614 Ciais, P., Wattenbach, M., Vuichard, N., Smith, P., Piao, S. L., Don, A., Luysaert, S., Janssens,
615 I. A., Bondeau, A., Dechow, R., Leip, A., Smith, P. C., Beer, C., van der Werf, G. R., Gervois,
616 S., Van Oost, K., Tomelleri, E., Freibauer, A., Schulze, E. D., and Team, C. S.: The European
617 carbon balance. Part 2: croplands, *Global Change Biol.*, 16, 1409-1428, doi: 10.1111/j.1365-
618 2486.2009.02055.x, 2010.

619 Ciais, P., Gervois, S., Vuichard, N., Piao, S. L., and Viovy, N.: Effects of land use change and
620 management on the European cropland carbon balance, *Global Change Biol.*, 17, 320-338,
621 doi: 10.1111/j.1365-2486.2010.02341.x, 2011.

622 Cristianini, N., and Shawe-Taylor, J.: *An Introduction to SupportVector Machines and Other*
623 *Kernel-Based Learning Methods*, Cambridge Univ. Press, Cambridge, UK, pp. 189, 2000.

624 Demyan, M. S., Ingwersen, J., Funkuin, Y. N., Ali, R. S., Mirzaeitalarposhti, R., Rasche, F.,
625 Poll, C., Muller, T., Streck, T., Kandeler, E., and Cadisch, G.: Partitioning of ecosystem
626 respiration in winter wheat and silage maize-modeling seasonal temperature effects, *Agric.*
627 *Ecosyst. Environ.*, 224, 131-144, doi: 10.1016/j.agee.2016.03.039, 2016.

628 de la Motte, L. G., Jérôme, E., Mamadou, O., Beckers, Y., Bodson, B., Heinesch, B., and
629 Aubinet, M.: Carbon balance of an intensively grazed permanent grassland in southern
630 Belgium, *Agric. For. Meteorol.*, 228-229, 370-383, doi: 10.1016/j.agrformet.2016.06.009,
631 2016.

632 Dold, C., Büyükçangaz, H., Rondinelli, W., Prueger, J., Sauer, T., and Hatfield, J.: Long-term
633 carbon uptake of agro-ecosystems in the Midwest, *Agric. For. Meteorol.*, 232, 128-140, doi:

634 10.1016/j.agrformet.2016.07.012, 2017.

635 Drewniak, B. A., Mishra, U., Song, J., Prell, J., and Kotamarthi, V. R.: Modeling the impact of
636 agricultural land use and management on US carbon budgets, *Biogeosciences*, 12, 2119-
637 2129, doi: 10.5194/bg-12-2119-2015, 2015.

638 Eichelmann, E., Wagner-Riddle, C., Warland, J., Deen, B., and Voroney, P.: Comparison of
639 carbon budget, evapotranspiration, and albedo effect between the biofuel crops switchgrass
640 and corn, *Agric. Ecosyst. Environ.*, 231, 271-282, doi: 10.1016/j.agee.2016.07.007, 2016.

641 Ekblad, A., Bostrom, B., Holm, A., and Comstedt, D.: Forest soil respiration rate and $\delta^{13}\text{C}$ is
642 regulated by recent above ground weather conditions, *Oecologia*, 143, 136-142, doi:
643 10.1007/s00442-004-1776-z, 2005.

644 Eugster, W., Moffat, A. M., Ceschia, E., Aubinet, M., Ammann, C., Osborne, B., Davis, P. A.,
645 Smith, P., Jacobs, C., Moors, E., Le Dantec, V., Beziat, P., Saunders, M., Jans, W., Grunwald,
646 T., Rebmann, C., Kutsch, W. L., Czerny, R., Janous, D., Moureaux, C., Dufranne, D., Carrara,
647 A., Magliulo, V., Di Tommasi, P., Olesen, J. E., Schelde, K., Olioso, A., Bernhofer, C.,
648 Cellier, P., Larmanou, E., Loubet, B., Wattenbach, M., Marloie, O., Sanz, M. J., Sogaard,
649 H., and Buchmann, N.: Management effects on European cropland respiration, *Agric.*
650 *Ecosyst. Environ.*, 139, 346-362, doi: 10.1016/j.agee.2010.09.001, 2010.

651 Falkowski, P., Scholes, R. J., Boyle, E. E. A., Canadell, J., Canfield, D., Elser, J., Gruber, N.,
652 Hibbard, K., Högberg, P., Linder, S., and Mackenzie, F. T.: The global carbon cycle: a test
653 of our knowledge of earth as a system, *Science*, 290, 291-296, doi:
654 10.1126/science.290.5490.291, 2000.

655 Falge, E., Baldocchi, D., Olson, R., Anthoni, P., Aubinet, M., Bernhofer, C., Burba, G.,

656 Ceulemans, R., Clement, R., Dolman, H., Granier, A., Gross, P., Grunwald, T., Hollinger,
657 D., Jensen, N. O., Katul, G., Keronen, P., Kowalski, A., Lai, C. T., Law, B. E., Meyers, T.,
658 Moncrieff, H., Moors, E., Munger, J. W., Pilegaard, K., Rannik, U., Rebmann, C., Suyker,
659 A., Tenhunen, J., Tu, K., Verma, S., Vesala, T., Wilson, K., and Wofsy, S.: Gap filling
660 strategies for defensible annual sums of net ecosystem exchange, *Agric. For. Meteorol.*, 107,
661 43-69, doi: 10.1016/S0168-1923(00)00225-2, 2001.

662 Falge, E., Baldocchi, D., Tenhunen, J., Aubinet, M., Bakwin, P., Berbigier, P., Bernhofer, C.,
663 Burba, G., Clement, R., Davis, K. J., Elbers, J. A., Goldstein, A. H., Grelle, A., Granier, A.,
664 Guomundsson, J., Hollinger, D., Kowalski, A. S., Katul, G., Law, B. E., Malhi, Y., Meyers,
665 T., Monson, R. K., Munger, J. W., Oechel, W., Paw, K. T., Pilegaard, K., Rannik, U.,
666 Rebmann, C., Suyker, A., Valentini, R., Wilson, K., and Wofsy, S.: Seasonality of ecosystem
667 respiration and gross primary production as derived from FLUXNET measurements, *Agric.*
668 *For. Meteorol.*, 113, 53-74, doi: 10.1016/S0168-1923(02)00102-8, 2002a.

669 Falge, E., Tenhunen, J., Baldocchi, D., Aubinet, M., Bakwin, P., Berbigier, P., Bernhofer, C.,
670 Bonnefond, J. M., Burba, G., Clement, R., Davis, K. J., Elbers, J. A., Falk, M., Goldstein, A.
671 H., Grelle, A., Granier, A., Grunwald, T., Gudmundsson, J., Hollinger, D., Janssens, I. A.,
672 Keronen, P., Kowalski, A. S., Katul, G., Law, B. E., Malhi, Y., Meyers, T., Monson, R. K.,
673 Moors, E., Munger, J. W., Oechel, W., U, K. T. P., Pilegaard, K., Rannik, U., Rebmann, C.,
674 Suyker, A., Thorgeirsson, H., Tirone, G., Turnipseed, A., Wilson, K., and Wofsy, S.: Phase
675 and amplitude of ecosystem carbon release and uptake potentials as derived from FLUXNET
676 measurements, *Agric. For. Meteorol.*, 113, 75-95, doi: 10.1016/S0168-1923(02)00103-X,
677 2002b.

678 Fargione, J. E., Bassett, S., Boucher, T., Bridgham, S. D., Conant, R. T., Cook-Patton, S. C.,
679 Ellis, P. W., Falcucci, A., Fourqurean, J. W., Gopalakrishna, T., Gu, H., Henderson, B.,
680 Hurteau, M. D., Kroeger, K. D., Kroeger, T., Lark, T. J., Leavitt, S. M., Lomax, G.,
681 McDonald, R. I., Megonigal, J. P., Miteva, D. A., Richardson, C. J., Sanderman, J., Shoch,
682 D., Spawn, S. A., Veldman, J. W., Williams, C. A., Woodbury, P. B., Zganjar, C., Baranski,
683 M., Elias, P., Houghton, R. A., Landis, E., McGlynn, E., Schlesinger, W. H., Siikamaki, J.
684 V., Sutton-Grier, A. E., and Griscom, B. W.: Natural climate solutions for the United States,
685 *Sci Adv*, 4, doi: 10.1126/sciadv.aat1869, 2018.

686 Fleisher, D. H., Timlin, D. J., and Reddy, V. R.: Elevated carbon dioxide and water stress effects
687 on potato canopy gas exchange, water use, and productivity, *Agric. For. Meteorol.*, 148,
688 1109-1122, doi: 10.1016/j.agrformet.2008.02.007, 2008.

689 Forkel, M., Carvalhais, N., Rödenbeck, C., Keeling, R., Heimann, M., Thonicke, K., Zaehle, S.,
690 and Reichstein, M.: Enhanced seasonal CO₂ exchange caused by amplified plant productivity
691 in northern ecosystems, *Science*, 351, 696-699, doi: 10.1126/science.aac4971, 2016.

692 Freibauer, A., Rounsevell, M. D. A., Smith, P., and Verhagen, J.: Carbon sequestration in the
693 agricultural soils of Europe, *Geoderma*, 122, 1-23, 10.1016/j.geoderma.2004.01.021, 2004.

694 Gao, X., Gu, F., Hao, W., Mei, X., Li, H., Gong, D., and Zhang, Z.: Carbon budget of a rainfed
695 spring maize cropland with straw returning on the Loess Plateau, China, *Science of The Total*
696 *Environment*, 586, 1193-1203, 10.1016/j.scitotenv.2017.02.113, 2017.

697 Gilmanov, T. G., Verma, S. B., Sims, P. L., Meyers, T. P., Bradford, J. A., Burba, G. G., and
698 Suyker, A. E.: Gross primary production and light response parameters of four Southern
699 Plains ecosystems estimated using long-term CO₂-flux tower measurements, *Global*

700 Biogeochem. Cycles, 17, Artn 1071, doi: 10.1029/2002gb002023, 2003.

701 Grant, R. F., Arkebauer, T. J., Dobermann, A., Hubbard, K. G., Schimelfenig, T. T., Suyker, A.
702 E., Verma, S. B., and Walters, D. T.: Net biome productivity of irrigated and rainfed maize-
703 soybean rotations: Modeling vs. measurements, *Agron. J.*, 99, 1404-1423, doi:
704 10.2134/agronj2006.0308, 2007.

705 Gray, J. M., Frohling, S., Kort, E. A., Ray, D. K., Kucharik, C. J., Ramankutty, N., and Friedl,
706 M. A.: Direct human influence on atmospheric CO₂ seasonality from increased cropland
707 productivity, *Nature*, 515, 398-401, doi: 10.1038/nature13957, 2014.

708 Griscom, B. W., Adams, J., Ellis, P. W., Houghton, R. A., Lomax, G., Miteva, D. A., Schlesinger,
709 W. H., Shoch, D., Siikamaki, J. V., Smith, P., Woodbury, P., Zganjar, C., Blackman, A.,
710 Campari, J., Conant, R. T., Delgado, C., Elias, P., Gopalakrishna, T., Hamsik, M. R., Herrero,
711 M., Kiesecker, J., Landis, E., Laestadius, L., Leavitt, S. M., Minnemeyer, S., Polasky, S.,
712 Potapov, P., Putz, F. E., Sanderman, J., Silvius, M., Wollenberg, E., and Fargione, J.: Natural
713 climate solutions, *P. Natl. Acad. Sci. USA*, 114, 11645-11650, doi:
714 10.1073/pnas.1710465114, 2017.

715 Heimann, M., and Reichstein, M.: Terrestrial ecosystem carbon dynamics and climate
716 feedbacks, *Nature*, 451, 289-292, doi: 10.1038/Nature06591, 2008.

717 Hollinger, S. E., Bernacchi, C. J., and Meyers, T. P.: Carbon budget of mature no-till ecosystem
718 in North Central Region of the United States, *Agric. For. Meteorol.*, 130, 59-69, doi:
719 10.1016/j.agrformet.2005.01.005, 2005.

720 Hsieh, C. I., Katul, G., and Chi, T.: An approximate analytical model for footprint estimation
721 of scalar fluxes in thermally stratified atmospheric flows, *Adv. Water Resour.*, 23, 765-772,

722 doi: 10.1016/S0309-1708(99)00042-1, 2000.

723 Huang, Y., Zhang, W., Sun, W. J., and Zheng, X. H.: Net primary production of Chinese
724 croplands from 1950 to 1999, *Ecol. Appl.*, 17, 692-701, doi: 10.1890/05-1792, 2007.

725 Hunt, J. E., Laubach, J., Barthel, M., Fraser, A., and Phillips, R. L.: Carbon budgets for an
726 irrigated intensively grazed dairy pasture and an unirrigated winter-grazed pasture,
727 *Biogeosciences*, 13, 2927-2944, doi: 10.5194/bg-13-2927-2016, 2016.

728 Hutchinson, J. J., Campbell, C. A., and Desjardins, R. L.: Some perspectives on carbon
729 sequestration in agriculture, *Agric. For. Meteorol.*, 142, 288-302, doi:
730 10.1016/j.agrformet.2006.03.030, 2007.

731 Iwasaki, H., Saito, H., Kuwao, K., Maximov, T. C., and Hasegawa, S.: Forest decline caused
732 by high soil water conditions in a permafrost region, *Hydrol. Earth Syst. Sc.*, 14, 301-307,
733 doi: 10.5194/hess-14-301-2010, 2010.

734 Jans, W. W. P., Jacobs, C. M. J., Kruijt, B., Elbers, J. A., Barendse, S., and Moors, E. J.: Carbon
735 exchange of a maize (*Zea mays* L.) crop: Influence of phenology, *Agric. Ecosyst. Environ.*,
736 139, 316-324, doi: 10.1016/j.agee.2010.06.008, 2010.

737 Kang, M., Ichii, K., Kim, J., Indrawati, Y. M., Park, J., Moon, M., Lim, J. H., and Chun, J. H.:
738 New gap-filling strategies for long-period flux data gaps using a data-driven approach,
739 *Atmosphere-Basel*, 10, doi: 10.3390/Atmos10100568, 2019.

740 Kendy, E., Gerard-Marchant, P., Walter, M. T., Zhang, Y. Q., Liu, C. M., and Steenhuis, T. S.:
741 A soil-water-balance approach to quantify groundwater recharge from irrigated cropland in
742 the North China Plain, *Hydrol. Process.*, 17, 2011-2031, doi: 10.1002/hyp.1240, 2003.

743 Kim, Y., Johnson, M.S., Knox, S.H., Black, T. A., Dalmagro, H. J., Kang, M., Kim, J.,

744 Baldocchi, D.: Gap-filling approaches for eddy covariance methane fluxes: A comparison of
745 three machine learning algorithms and a traditional method with principal component
746 analysis. *Global Change Biol.*, 26, 1-20 doi: 10.1111/gcb.14845, 2019.

747 Kutsch, W. L., Aubinet, M., Buchmann, N., Smith, P., Osborne, B., Eugster, W., Wattenbach,
748 M., Schrumpf, M., Schulze, E. D., Tomelleri, E., Ceschia, E., Bernhofer, C., Beziat, P.,
749 Carrara, A., Di Tommasi, P., Grunwald, T., Jones, M., Magliulo, V., Marloie, O., Moureaux,
750 C., Olioso, A., Sanz, M. J., Saunders, M., Sogaard, H., and Ziegler, W.: The net biome
751 production of full crop rotations in Europe, *Agric. Ecosyst. Environ.*, 139, 336-345, doi:
752 10.1016/j.agee.2010.07.016, 2010.

753 Lal, R.: World cropland soils as a source or sink for atmospheric carbon, *Adv. Agron.*, 71, 145-
754 191, 2001.

755 Latimer, R. N. C. and Risk, D. A.: An inversion approach for determining distribution of
756 production and temperature sensitivity of soil respiration, *Biogeosciences*, 13, 2111-2122,
757 doi: 10.5194/bg-13-2111-2016, 2016.

758 Lei, H. M., and Yang, D. W.: Seasonal and interannual variations in carbon dioxide exchange
759 over a cropland in the North China Plain, *Global Change Biol.*, 16, 2944-2957, doi:
760 10.1111/j.1365-2486.2009.02136.x, 2010.

761 Lei, H. M., Yang, D. W., Cai, J. F., and Wang, F. J.: Long-term variability of the carbon balance
762 in a large irrigated area along the lower Yellow River from 1984 to 2006, *Sci. China Earth*
763 *Sci.*, 56, 671-683, doi: 10.1007/s11430-012-4473-5, 2013.

764 Li, J., Yu, Q., Sun, X. M., Tong, X. J., Ren, C. Y., Wang, J., Liu, E. M., Zhu, Z. L., and Yu, G.
765 R.: Carbon dioxide exchange and the mechanism of environmental control in a farmland

766 ecosystem in North China Plain, *Sci. China Ser. D*, 49, 226-240, doi: 10.1007/s11430-006-
767 8226-1, 2006.

768 Luo, Y., He, C. S., Sophocleous, M., Yin, Z. F., Ren, H. R., and Zhu, O. Y.: Assessment of
769 crop growth and soil water modules in SWAT2000 using extensive field experiment data in
770 an irrigation district of the Yellow River Basin, *J Hydrol*, 352, 139-156, doi:
771 10.1016/j.jhydrol.2008.01.003, 2008.

772 Mauder, M., and Foken, T.: Documentation and instruction manual of the eddy covariance
773 software package TK2. Universität Bayreuth, Abt. Mikrometeorologie, Arbeitsergebnisse,
774 2004.

775 Mauder, M., and Foken, T.: Documentation and instruction manual of the eddy-covariance
776 software package TK3, Universität Bayreuth, Abt. Mikrometeorologie, Arbeitsergebnisse
777 2011.

778 Moureaux, C., Debacq, A., Bodson, B., Heinesch, B., and Aubinet, M.: Annual net ecosystem
779 carbon exchange by a sugar beet crop, *Agric. For. Meteorol.*, 139, 25-39, doi:
780 10.1016/j.agrformet.2006.05.009, 2006.

781 Moureaux, C., Debacq, A., Hoyaux, J., Suleau, M., Tourneur, D., Vancutsem, F., Bodson, B.,
782 and Aubinet, M.: Carbon balance assessment of a Belgian winter wheat crop (*Triticum*
783 *aestivum* L.), *Global Change Biol.*, 14, 1353-1366, doi: 10.1111/j.1365-2486.2008.01560.x,
784 2008.

785 National Standards of Environmental Protection of the People's Republic of China: Soil –
786 Determination of organic carbon – Combustion oxidation-titration method. HJ658-2013,
787 2013.

788 Özdoğan, M.: Exploring the potential contribution of irrigation to global agricultural primary
789 productivity, *Global Biogeochem. Cycles*, 25, doi: 10.1029/2009GB003720, 2011.

790 Phillips, C. L., Nickerson, N., Risk, D. and Bond, B. J.: Interpreting diel hysteresis between soil
791 respiration and temperature, *Global Change Biol.*, 17, 515-527, doi: 10.1111/j.1365-
792 2486.2010.02250.x, 2011.

793 Piao, S. L., Ito, A., Li, S. G., Huang, Y., Ciais, P., Wang, X. H., Peng, S. S., Nan, H. J., Zhao,
794 C., Ahlstrom, A., Andres, R. J., Chevallier, F., Fang, J. Y., Hartmann, J., Huntingford, C.,
795 Jeong, S., Levis, S., Levy, P. E., Li, J. S., Lomas, M. R., Mao, J. F., Mayorga, E., Mohammat,
796 A., Muraoka, H., Peng, C. H., Peylin, P., Poulter, B., Shen, Z. H., Shi, X., Sitch, S., Tao, S.,
797 Tian, H. Q., Wu, X. P., Xu, M., Yu, G. R., Viovy, N., Zaehle, S., Zeng, N., and Zhu, B.: The
798 carbon budget of terrestrial ecosystems in East Asia over the last two decades,
799 *Biogeosciences*, 9, 3571-3586, doi: 10.5194/bg-9-3571-2012, 2012.

800 Poorter, H., Niklas, K. J., Reich, P. B., Oleksyn, J., Poot, P., and Mommer, L.: Biomass
801 allocation to leaves, stems and roots: meta-analyses of interspecific variation and
802 environmental control, *New Phytol*, 193, 30-50, doi: 10.1111/j.1469-8137.2011.03952.x,
803 2012.

804 Poulter, B., Frank, D., Ciais, P., Myneni, R. B., Andela, N., Bi, J., Broquet, G., Canadell, J. G.,
805 Chevallier, F., Liu, Y. Y. and Running, S. W.: Contribution of semi-arid ecosystems to
806 interannual variability of the global carbon cycle, *Nature*, 509, 600-603,
807 doi:10.1038/nature13376, 2014.

808 Reichstein, M., Falge, E., Baldocchi, D., Papale, D., Aubinet, M., Berbigier, P., Bernhofer, C.,
809 Buchmann, N., Gilmanov, T., Granier, A., Grunwald, T., Havrankova, K., Ilvesniemi, H.,

810 Janous, D., Knohl, A., Laurila, T., Lohila, A., Loustau, D., Matteucci, G., Meyers, T.,
811 Miglietta, F., Ourcival, J. M., Pumpanen, J., Rambal, S., Rotenberg, E., Sanz, M., Tenhunen,
812 J., Seufert, G., Vaccari, F., Vesala, T., Yakir, D., and Valentini, R.: On the separation of net
813 ecosystem exchange into assimilation and ecosystem respiration: review and improved
814 algorithm, *Global Change Biol.*, 11, 1424-1439, doi: 10.1111/j.1365-2486.2005.001002.x,
815 2005.

816 Sauerbeck, D. R.: CO₂ emissions and C sequestration by agriculture - perspectives and
817 limitations, *Nutr. Cycl. Agroecosys.*, 60, 253-266, doi: 10.1023/A:1012617516477, 2001.

818 Schmidt, M., Reichenau, T. G., Fiener, P., and Schneider, K.: The carbon budget of a winter
819 wheat field: An eddy covariance analysis of seasonal and inter-annual variability, *Agric. For.*
820 *Meteorol.*, 165, 114-126, doi: 10.1016/j.agrformet.2012.05.012, 2012.

821 Shen, Y., Zhang, Y., Scanlon, B. R., Lei, H., Yang, D., and Yang, F: Energy/water budgets and
822 productivity of the typical croplands irrigated with groundwater and surface water in the
823 North China Plain, *Agric. For. Meteorol.*, 181, 133-142, doi:
824 10.1016/j.agrformet.2013.07.013, 2013.

825 Smith, P.: Carbon sequestration in croplands: the potential in Europe and the global context,
826 *Eur. J. Agron.*, 20, 229-236, doi: 10.1016/j.eja.2003.08.002, 2004.

827 Smith, P., Lanigan, G., Kutsch, W. L., Buchmann, N., Eugster, W., Aubinet, M., Ceschia, E.,
828 Beziat, P., Yeluripati, J. B., Osborne, B., Moors, E. J., Brut, A., Wattenbach, M., Saunders,
829 M., and Jones, M.: Measurements necessary for assessing the net ecosystem carbon budget
830 of croplands, *Agric. Ecosyst. Environ.*, 139, 302-315, doi: 10.1016/j.agee.2010.04.004, 2010.

831 Smith, W. K., Cleveland, C. C., Reed, S. C., and Running, S. W.: Agricultural conversion

832 without external water and nutrient inputs reduces terrestrial vegetation productivity,
833 *Geophys. Res. Lett.*, 41, 449-455, doi: 10.1002/2013GL058857, 2014.

834 Suyker, A.E., Verma, S. B., Burba, G. G., and Arkebauer, T. J., Gross primary production and
835 ecosystem respiration of irrigated maize and irrigated soybean during a growing season.
836 *Agric. For. Meteorol.*, 31, 180-190, doi: 10.1016/j.agrformet.2005.05.007, 2005.

837 Suleau, M., Moureaux, C., Dufranne, D., Buysse, P., Bodson, B., Destain, J. P., Heinesch, B.,
838 Debacq, A., and Aubinet, M.: Respiration of three Belgian crops: Partitioning of total
839 ecosystem respiration in its heterotrophic, above- and below-ground autotrophic components,
840 *Agric. For. Meteorol.*, 151, 633-643, doi: 10.1016/j.agrformet.2011.01.012, 2011.

841 Taylor, A. M., Amiro, B. D., and Fraser, T. J.: Net CO₂ exchange and carbon budgets of a three-
842 year crop rotation following conversion of perennial lands to annual cropping in Manitoba,
843 Canada, *Agric. For. Meteorol.*, 182–183, 67-75, doi: 10.1016/j.agrformet.2013.07.008, 2013.

844 Terazawa, K., Maruyama, Y., and Morikawa, Y.: Photosynthetic and Stomatal Responses of
845 *Larix-Kaempferi* Seedlings to Short-Term Waterlogging, *Ecol. Res.*, 7, 193-197, doi:
846 10.1007/Bf02348500, 1992.

847 Tian, H., Melillo, J., Kicklighter, D., McGuire, A., and Helfrich, J.: The sensitivity of terrestrial
848 carbon storage to historical climate variability and atmospheric CO₂ in the United States,
849 *Tellus B*, 51, 414-452, 1999.

850 Ueyama, M., Ichii, K., Iwata, H., Euskirchen, E. S., Zona, D., Rocha, A. V., Harazono, Y.,
851 Iwama, C., Nakai, T., and Oechel, W. C.: Upscaling terrestrial carbon dioxide fluxes in
852 Alaska with satellite remote sensing and support vector regression, *J. Geophys. Res-Biogeo.*,
853 118, 1266-1281, doi: 10.1002/jgrg.20095, 2013.

854 van Wesemael, B., Paustian, K., Meersmans, J., Goidts, E., Barancikova, G., and Easter, M.:
855 Agricultural management explains historic changes in regional soil carbon stocks, *P. Natl.*
856 *Acad. Sci. USA*, 107, 14926-14930, doi: 10.1073/pnas.1002592107, 2010.

857 Verma, S. B., Dobermann, A., Cassman, K. G., Walters, D. T., Knops, J. M., Arkebauer, T. J.,
858 Suyker, A. E., Burba, G. G., Amos, B., Yang, H. S., Ginting, D., Hubbard, K. G., Gitelson,
859 A. A., and Walter-Shea, E. A.: Annual carbon dioxide exchange in irrigated and rainfed
860 maize-based agroecosystems, *Agric. For. Meteorol.*, 131, 77-96, doi:
861 10.1016/j.agrformet.2005.05.003, 2005.

862 Vick, E. S. K., Stoy, P. C., Tang, A. C. I., and Gerken, T.: The surface-atmosphere exchange of
863 carbon dioxide, water, and sensible heat across a dryland wheat-fallow rotation, *Agric.*
864 *Ecosyst. Environ.*, 232,129-140, doi: 10.1016/j.agee.2016.07.018, 2016.

865 Wang, Y. Y., Hu, C. S., Dong, W. X., Li, X. X., Zhang, Y. M., Qin, S. P., and Oenema, O.:
866 Carbon budget of a winter-wheat and summer-maize rotation cropland in the North China
867 Plain, *Agric. Ecosyst. Environ.*, 206, 33-45, doi: 10.1016/j.agee.2015.03.016, 2015.

868 Wolf, J., West, T. O., Le Page, Y., Kyle, G. P., Zhang, X., Collatz, G. J., and Imhoff, M. L.:
869 Biogenic carbon fluxes from global agricultural production and consumption, *Global*
870 *Biogeochem. Cy.*, 29, 1617-1639, doi: 10.1002/2015gb005119, 2015.

871 Zhang, Q., Lei, H. M., and Yang, D. W.: Seasonal variations in soil respiration, heterotrophic
872 respiration and autotrophic respiration of a wheat and maize rotation cropland in the North
873 China Plain, *Agric. For. Meteorol.*, 180, 34-43, doi: 10.1016/j.agrformet.2013.04.028, 2013.

874 Zhang, Q., Katul, G. G., Oren, R., Daly, E., Manzoni, S., and Yang, D. W.: The hysteresis
875 response of soil CO₂ concentration and soil respiration to soil temperature, *J. Geophys. Res-*

876 Biogeo., 120, 1605-1618, doi: 10.1002/2015JG003047, 2015a.

877 Zhang, Q., Lei, H.M., Yang, D.W., Bo H. B., and Cai, J. F.: On the diel characteristics of soil
878 respiration over the North China Plain, J. Tsinghua University (Science and Technology),
879 55, 33-38, 2015b. (in Chinese with English abstract)

880 Zhang, Q., Phillips, R.P., Manzoni, S., Scott, R.L., Oishi, A.C., Finzi, A., Daly, E., Vargas, R.
881 and Novick, K.A.: Changes in photosynthesis and soil moisture drive the seasonal soil
882 respiration-temperature hysteresis relationship. Agric. For. Meteorol., 259:184-195, doi:
883 10.1016/j.agrformet.2018.05.005, 2018.

884 Zhang, Y. Q., Yu, Q., Jiang, J., and Tang, Y. H.: Calibration of Terra/MODIS gross primary
885 production over an irrigated cropland on the North China Plain and an alpine meadow on the
886 Tibetan Plateau, Global Change Biol., 14, 757-767, doi: 10.1111/j.1365-2486.2008.01538.x,
887 2008.

888 Zhao, M. S., Heinsch, F. A., Nemani, R. R., and Running, S. W.: Improvements of the MODIS
889 terrestrial gross and net primary production global data set, Remote Sens. Environ., 95,
890 164-176, doi: 10.1016/j.rse.2004.12.011, 2005.

891 **Tables and figures**

892

Table 1 Carbon content of different parts (gC kg⁻¹ DM)

crop	date	root	stem	green leaf	dead leaf	grain
wheat	3/15/2011	416	413	488	-	-
	3/22/2011	454	-	476	-	-
	3/29/2011	-	436	451	-	-
	4/5/2011	527	431	534	-	-
	4/13/2011	348	417	457	-	-
	4/21/2011	434	415	522	-	-
	4/29/2011	410	443	510	-	-
	5/6/2011	434	423	481	-	-
	5/14/2011	275	445	485	-	-
	5/22/2011	380	474	-	538	470
	5/29/2011	461	515	503	444	479
	6/5/2011	393	432	439	400	432
6/10/2011	393	429	-	426	449	
maize	7/4/2011	339	351	476	-	-
	7/13/2011	370	392	455	-	-
	7/21/2011	389	418	463	-	-
	7/29/2011	406	432	462	-	-
	8/5/2011	399	429	481	-	-
	8/12/2011	443	439	469	-	-
	8/22/2011	403	462	469	-	-
	9/3/2011	386	466	499	-	446
	9/11/2011	466	465	505	-	460
	9/20/2011	445	481	481	-	454
	9/30/2011	439	481	489	457	462

893

Table 2 Various ratios associated with carbon fluxes in croplands

crop species	ER/GPP	R _A /GPP ^a	R _H /ER	R _{AB} /ER	R _{AA} /ER	source
maize	0.69	0.32	0.54	0.21	0.25	this study
maize	0.67	0.56	0.16	0.25	0.59	Jans et al. (2010)
maize	0.85	0.45	0.47	0.02	0.51	Wang et al. (2015)
maize	0.80	0.65	0.19	0.21	0.60	Demyan et al. (2016) ^b
wheat	0.59	0.24	0.59	0.21	0.20	this study
wheat	0.71	0.49	0.31	0.19	0.50	Demyan et al. (2016) ^b
wheat	0.61	0.46	0.24	0.31	0.45	Moureaux et al. (2008)
wheat (2005)	0.60	0.44	0.26		0.74	Aubinet et al. (2009) ^c
wheat (2007)	0.57	0.48	0.15		0.85	Aubinet et al. (2009) ^c
wheat	0.57	0.45	0.21	0.17	0.62	Suleau et al. (2011)
wheat	0.66	0.43	0.35	0.05	0.59	Wang et al. (2015)
potato	0.48	0.37	0.24		0.76	Aubinet et al. (2009) ^c
potato	0.47	0.32	0.33	0.14	0.53	Suleau et al. (2011)
sugar beet	0.44	0.30	0.31		0.69	Aubinet et al. (2009) ^c
sugar beet	0.36	0.22	0.37	0.25	0.36	Suleau et al. (2011)

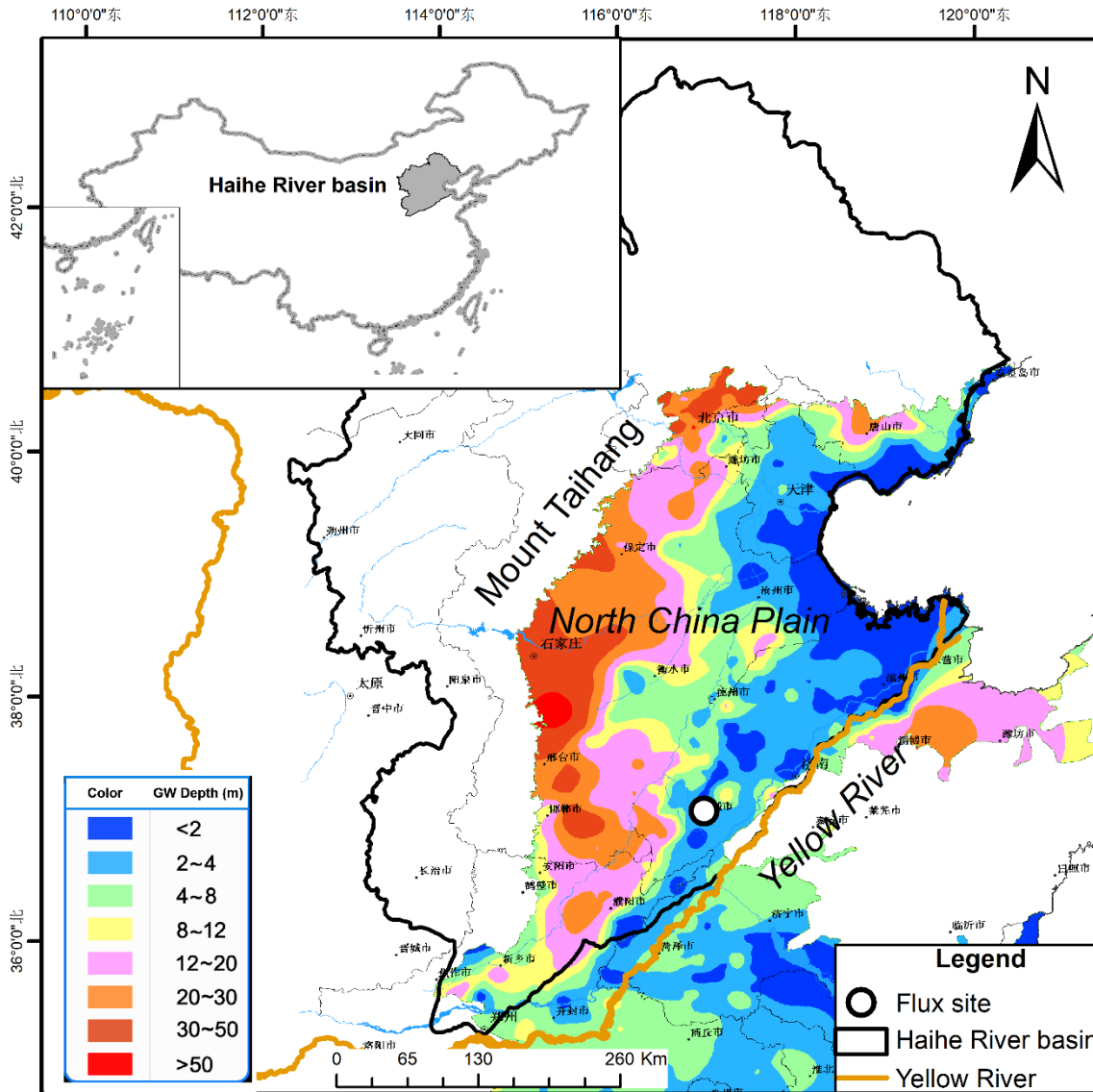
895 Note:

896 a- the values in parentheses indicate that the value is calculated by the equation $R_A/GPP=1-NPP/GPP$.

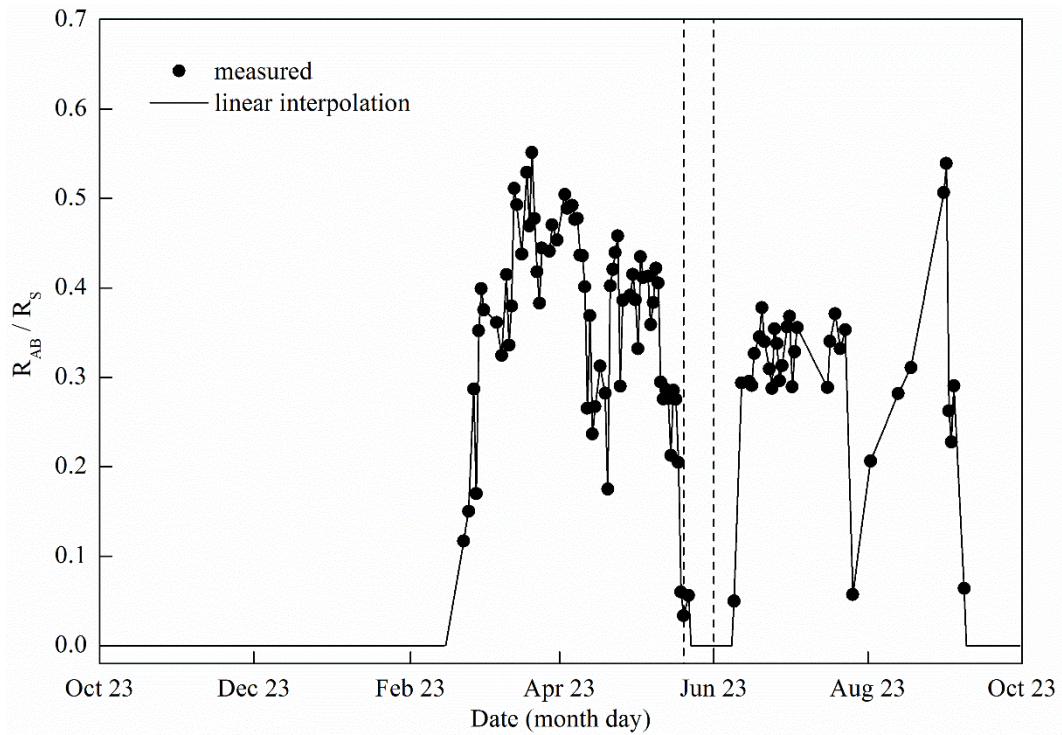
897 b- The data was from 2012, and the estimation is based on the average of the static and dynamic methods

898 c- R_A as well as R_H is the averaged values of their two corresponding methods

899



900
 901 Fig. 1 Location of the experimental site. The background is the shallow groundwater depth in
 902 early September of 2011 (modified from <http://dxs.hydroinfo.gov.cn/shuiziyuan/>)



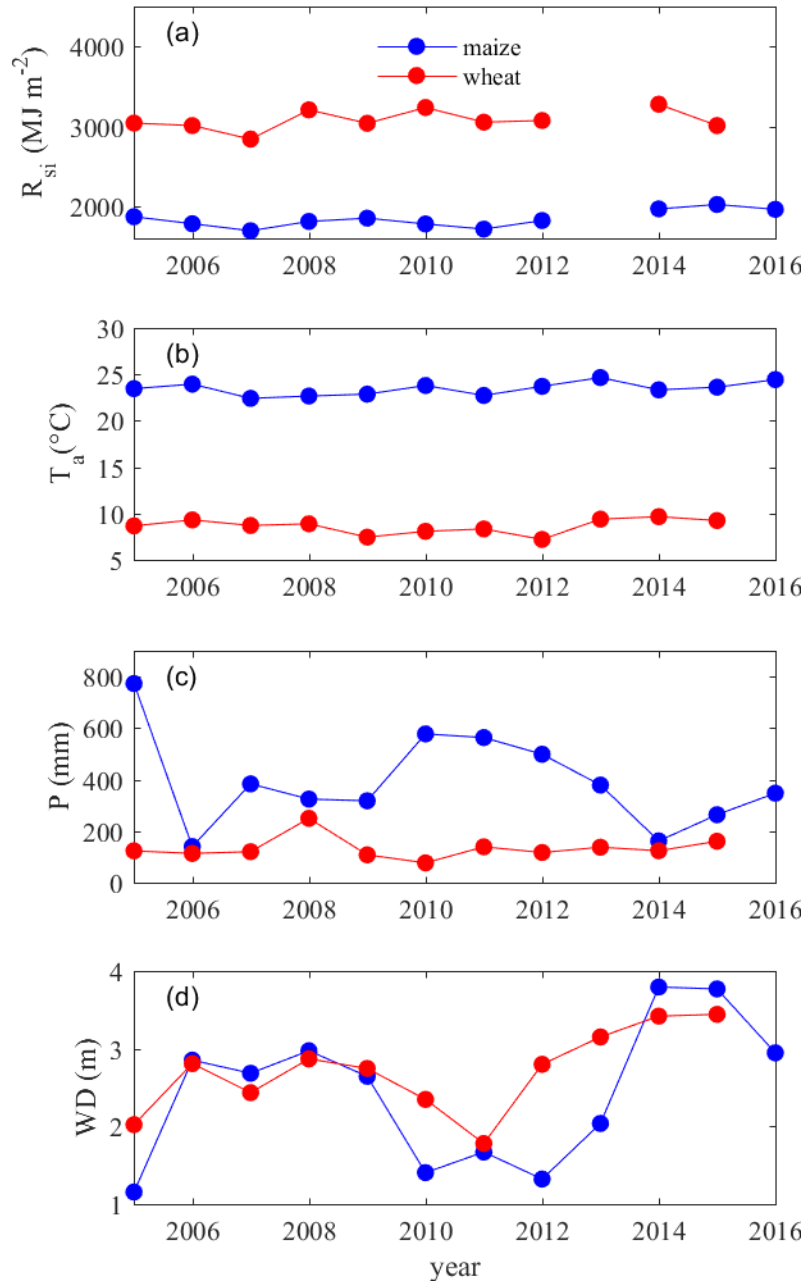
903

904

905

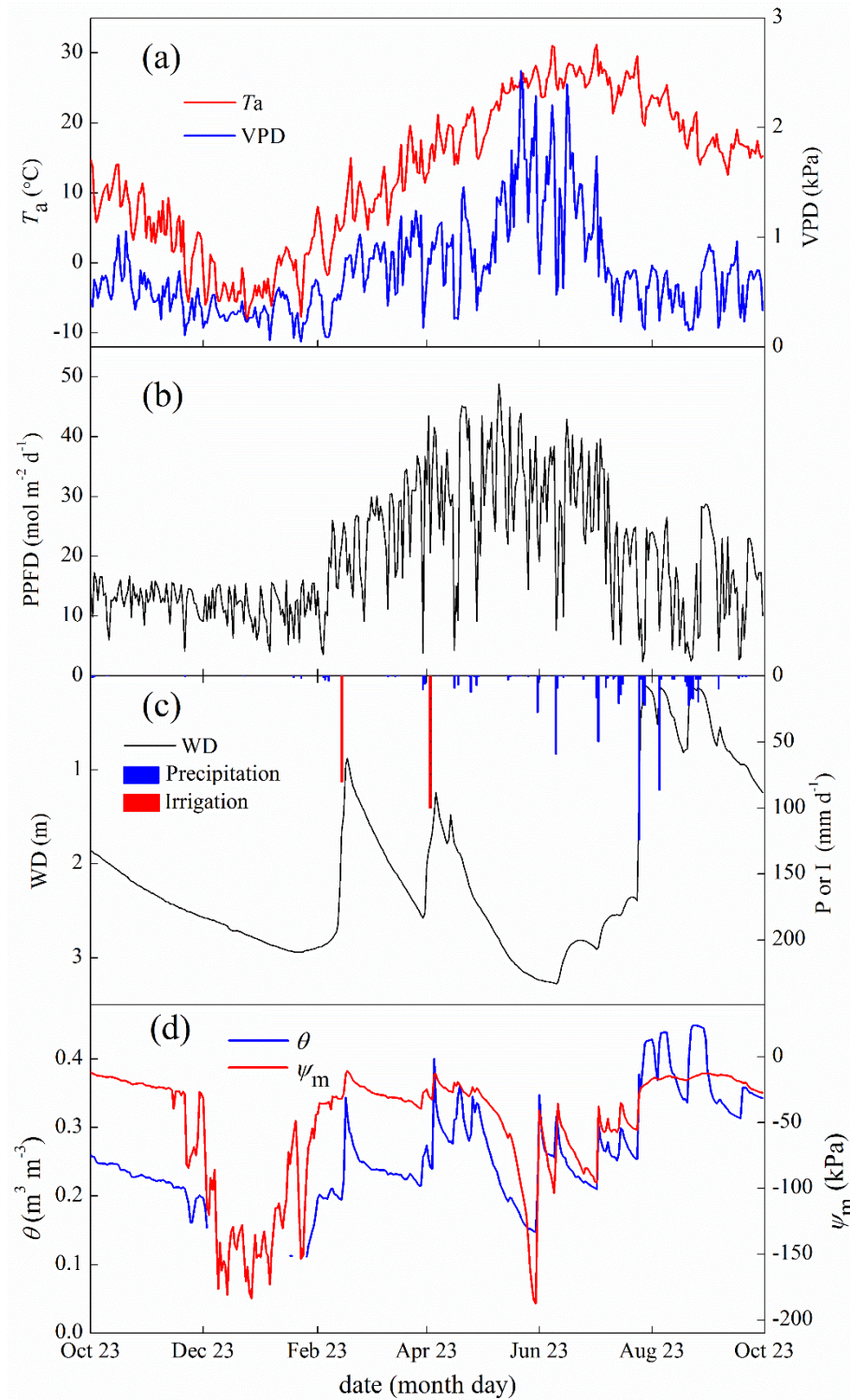
906

Fig. 2 Seasonal variations in the ratio of below-ground autotrophic respiration (R_{AB}) to total soil respiration (R_S). Two vertical dashed lines (hereafter) represent the date of harvesting wheat and sowing maize, respectively.



907
 908
 909
 910
 911

Fig. 3 The seasonal (a) total incoming short-wave radiation (R_{si}), (b) average air temperature (T_a), (c) total precipitation (P) and (d) average groundwater depth (D) for both wheat and maize evaluated for the period from 2005 through 2016. Note that incoming short-wave radiation in the 2013 season was missing due to equipment malfunction.



912

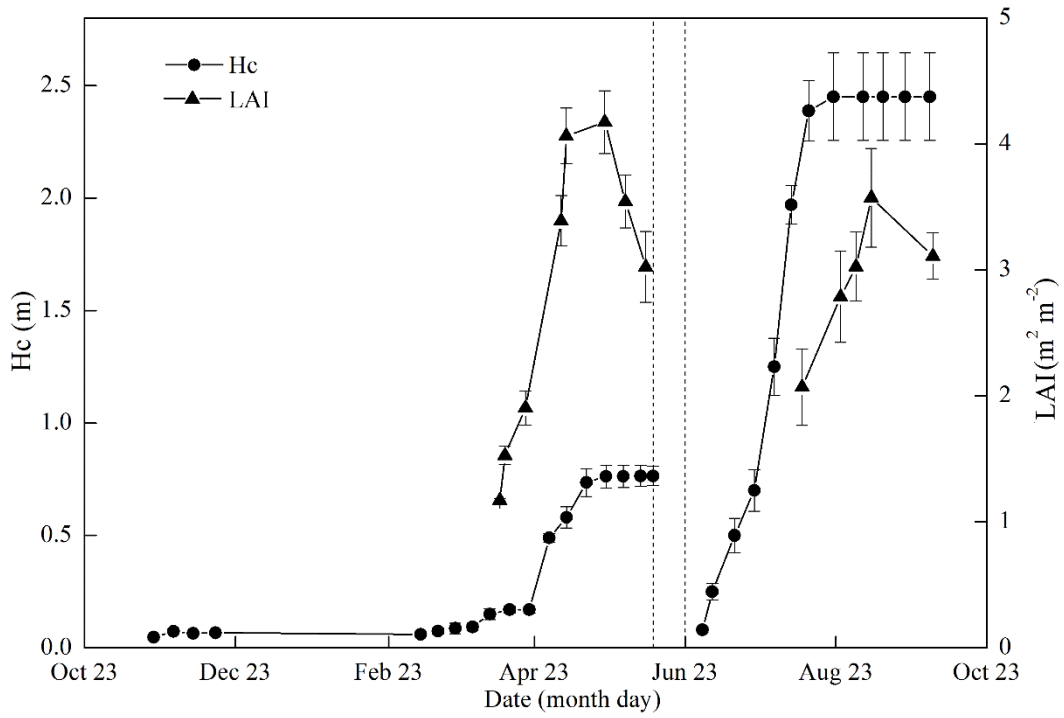
913

914

915

916

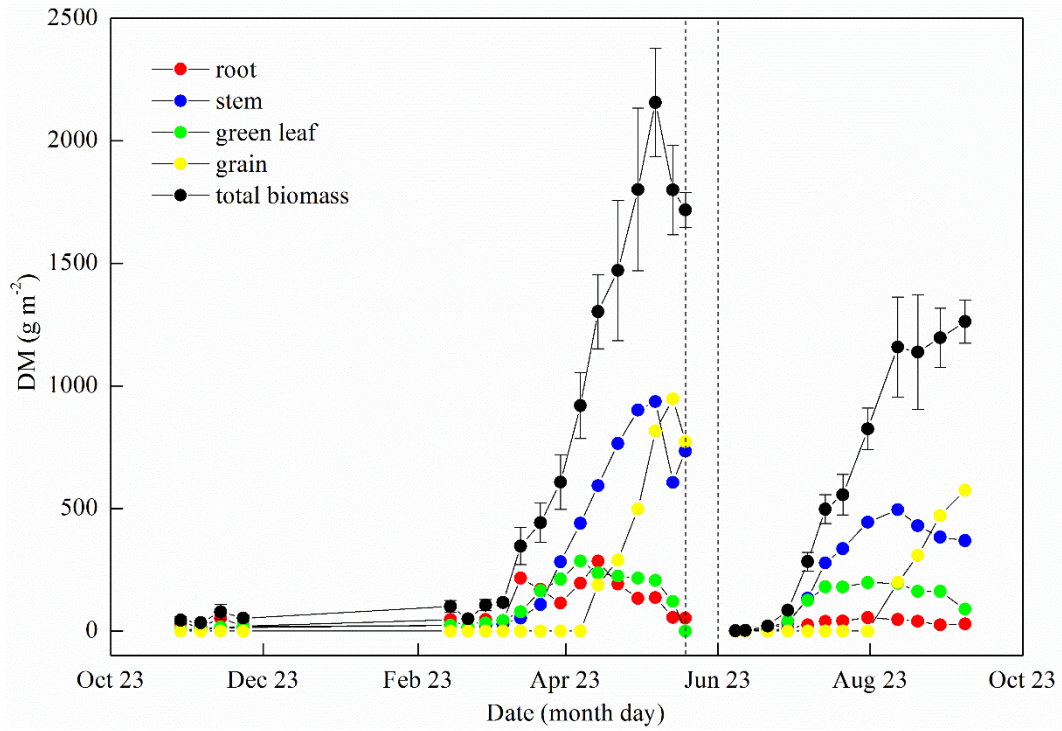
Fig. 4 Seasonal variations in the environmental variables of (a) air temperature (T_a), soil temperature at 5cm depth (T_s) and vapor pressure deficit (VPD), (b) photosynthetic photon flux density (PPFD), (c) precipitation (P), irrigation (I) and groundwater depth (WD), and (d) volumetric soil moisture (θ) and soil matric potential (ψ_m).



917

918 Fig. 5 Seasonal variations in canopy height (Hc) and leaf area index (LAI). The error bars

919 denote 1 standard deviation of the ten points.



920

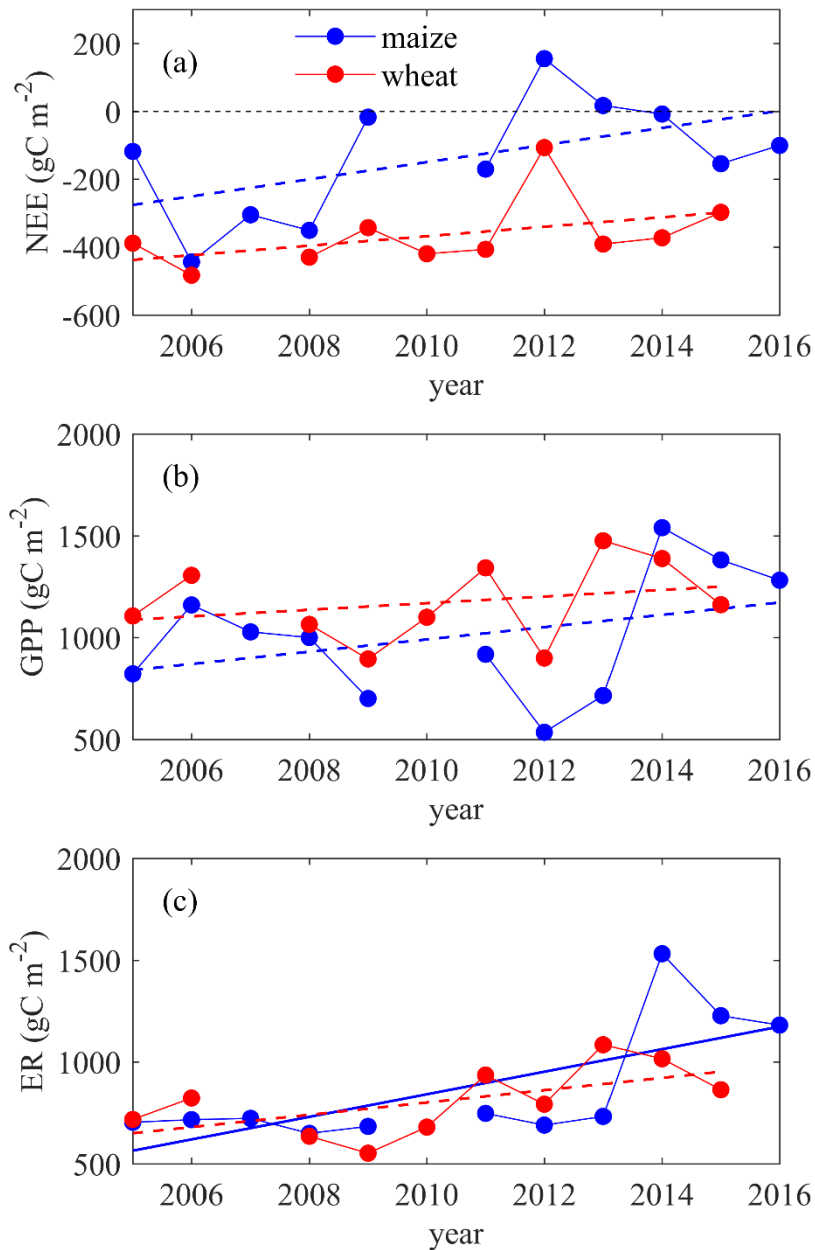
921

Fig. 6 Seasonal variations in the total dry biomass (DM) and its major parts of root, stem, green leaf and grain. The error bars of total biomass denote 1 standard deviation of the four

922

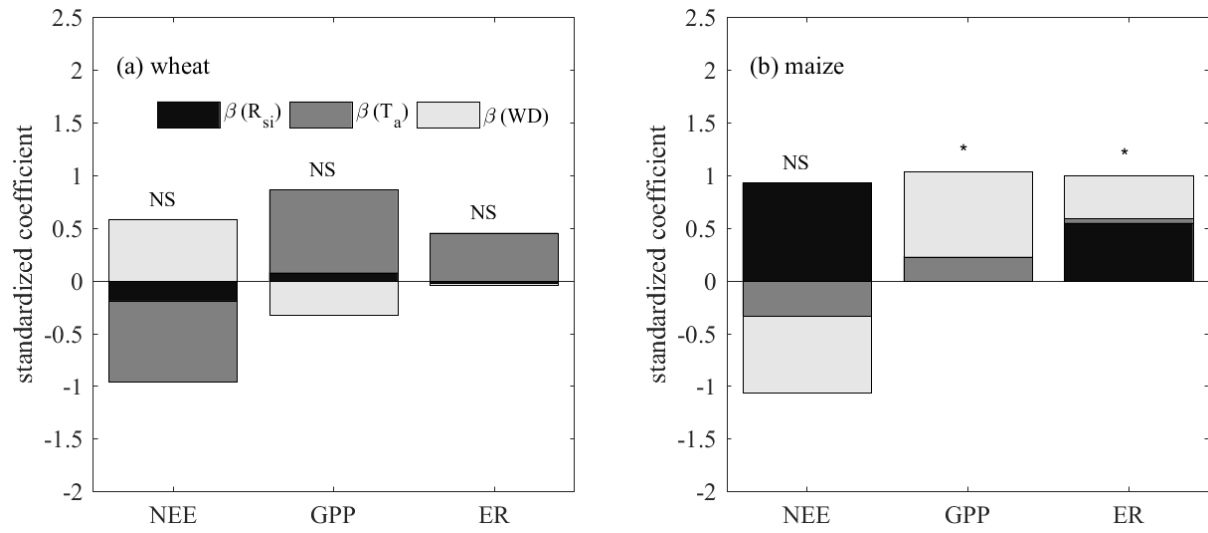
923

sample points.



924

925 Fig. 7 The temporal trend of annual (a) Net Ecosystem Exchange (NEE), (b) Gross Primary
 926 Productivity (GPP) and (c) Ecosystem Respiration (ER) for both wheat and maize from 2005
 927 through 2016. Note that though most gaps of carbon fluxes were filled, the wheat of 2007 was
 928 excluded as it had a large gap accounting for 26 % of annual records unable to fill; maize was
 929 not planted in the growing season of 2010. Note that the solid line represents the temporal
 930 trend passes F-test at $p < 0.05$ significance level, while the dashed line represents the temporal
 931 trend does not pass the F-test at $p < 0.05$ level.



932

933

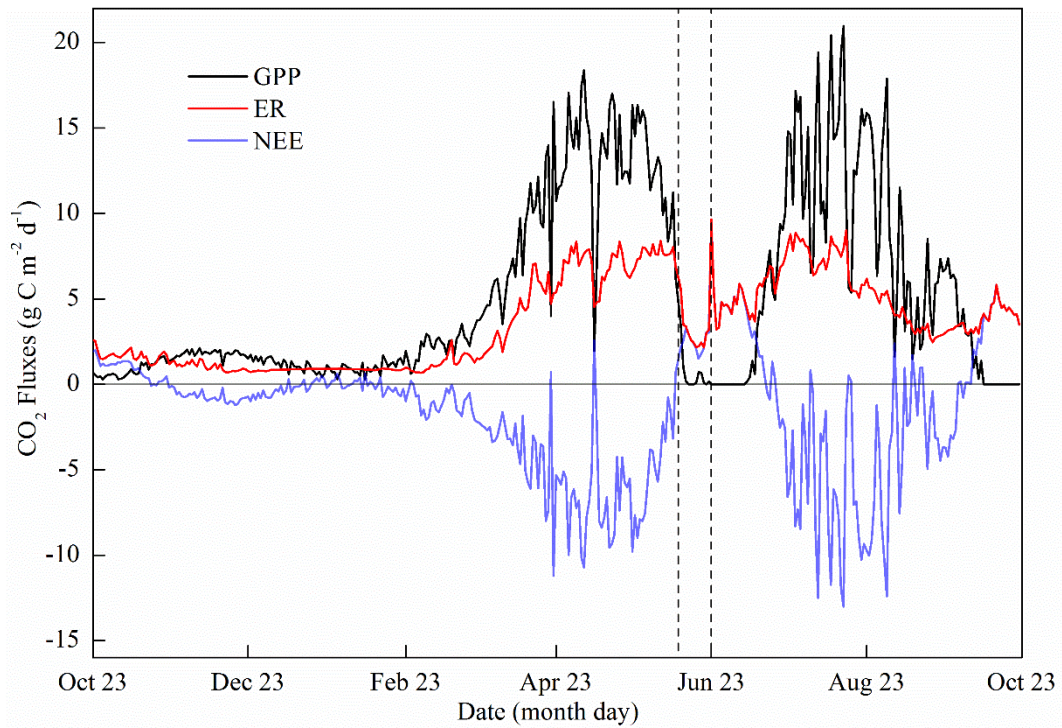
934

935

936

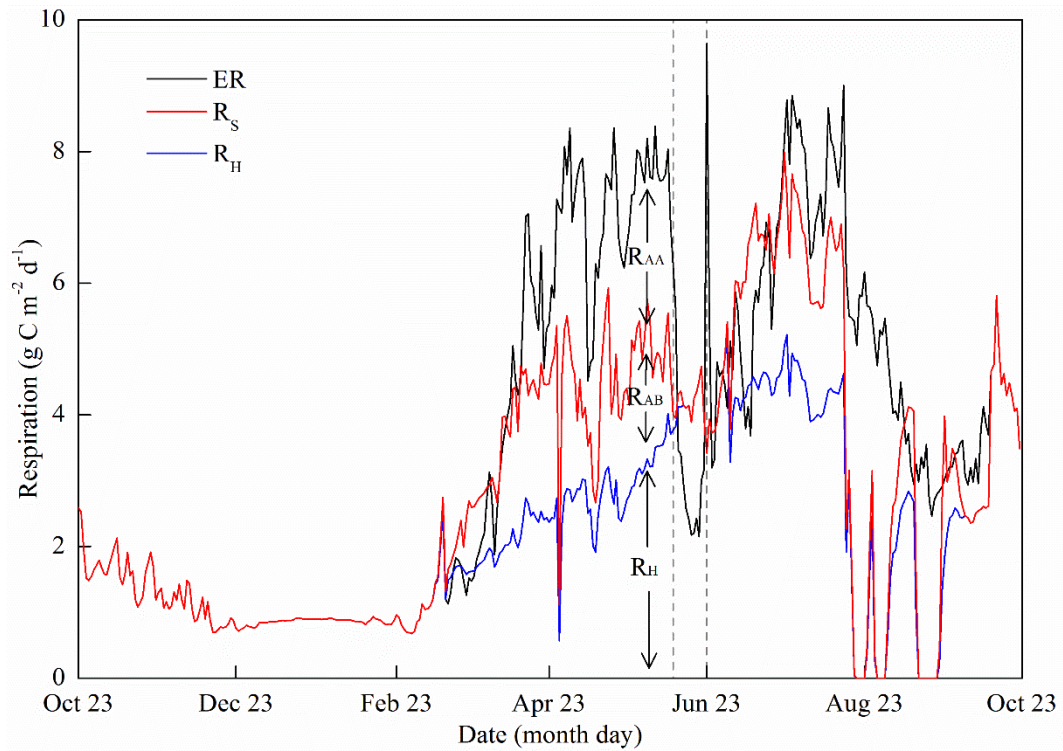
Fig. 8 The result of multiple regression for NEE, GPP and ER with incoming short-wave radiation (R_{si}), air temperature (T_a) and groundwater depth (WD) for both (a) wheat and (b) maize. Note that * denotes that the regression passes $p < 0.05$ significance level, and NS indicates non-significant.

937



938

939 Fig. 9 Seasonal variations in Gross Primary Productivity (GPP), Net Ecosystem Exchange
940 (NEE) and Ecosystem Respiration (ER) (those before April 2nd were calculated with SVR
941 method)



942

943

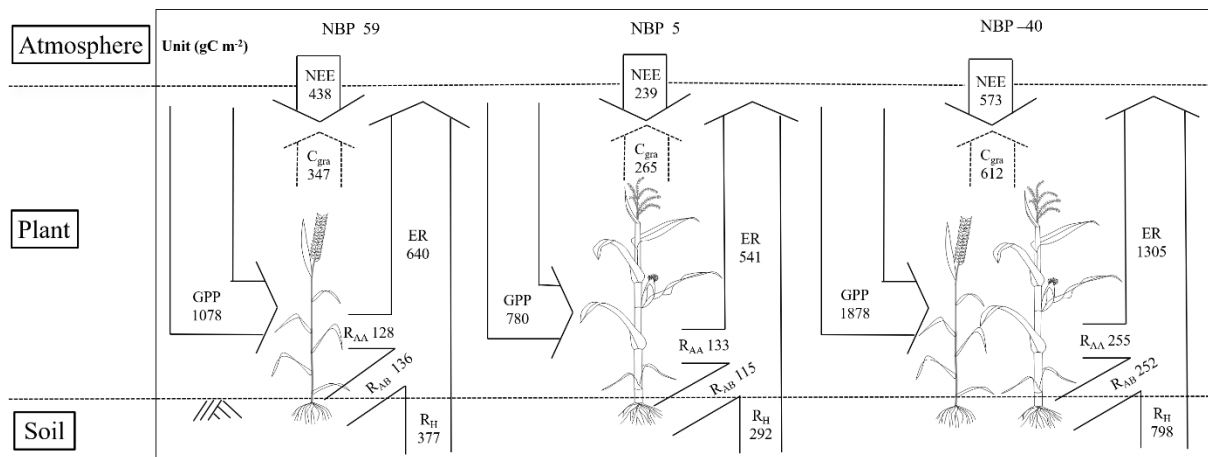
944

945

946

947

Fig. 10 Seasonal variations in the components of Ecosystem Respiration (ER), total soil respiration (R_S), soil heterotrophic respiration (R_H). The difference between ER and R_S denotes above-ground autotrophic respiration (R_{AA}), and the difference between R_S and R_H denotes below-ground autotrophic respiration (R_{AB}).



948

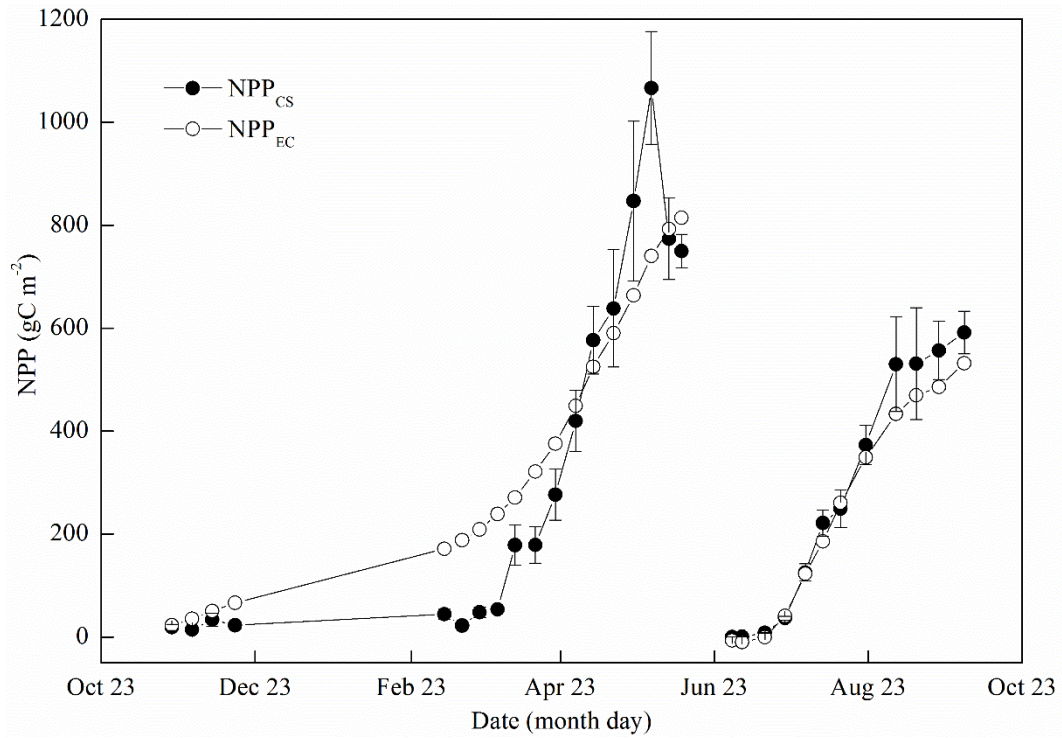
949

950

951

952

Fig. 11 Carbon budget of wheat (left), maize (middle) and the full wheat-maize rotation cycle with fallow periods included (right). Note that absolute value of NEE is shown here; NBPs of wheat and maize are the average of two independent methods (i.e, eddy covariance-based and crop sample-based)



953

954

955

956

Fig. 12 Seasonal variations in the cumulative Net Primary Productivity (NPP) with two independent methods of Crop Sample (NPP_{CS}) and Eddy Covariance (NPP_{EC}) complemented with soil respiration measurements.